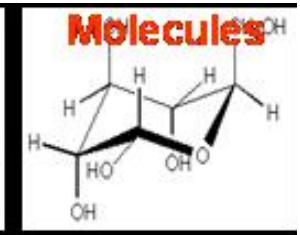
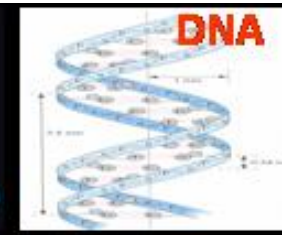
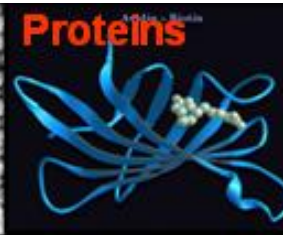
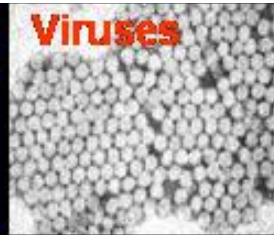
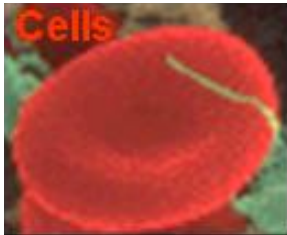


Key Topics

- Biochips/Biosensors and Device Fabrication
- Cells, DNA, Proteins
- **Micro-fluidics**
- **Biochip Sensors & Detection Methods**
- Micro-arrays
- Lab-on-a-chip Devices



Continuous Fluid Flows

Navier Stokes Equation (dimensional form)

$$\rho \frac{D\vec{V}}{Dt} = \rho \frac{\partial \vec{V}}{\partial t} + \rho (\vec{V} \cdot \nabla) \vec{V} = \rho \vec{g} - \nabla p + \mu \nabla^2 \vec{V}$$

Scale equation:

$$V = u\vec{V}'; \bar{x} = Lx'; p = \frac{\mu u}{L} p'; t = \frac{L}{u} t'$$

$$\text{Re} \frac{D\vec{V}}{Dt} = \text{Re} \left(\frac{\partial \vec{V}}{\partial t} + (\vec{V} \cdot \nabla) \vec{V} \right) = \text{Re} \cdot Fr^{-2} \frac{\vec{g}}{|\vec{g}|} - \nabla p + \nabla^2 \vec{V}$$

$$\text{where } \text{Re} = \frac{\rho u L}{\mu}, Fr^{-2} = \frac{gL}{u^2}$$

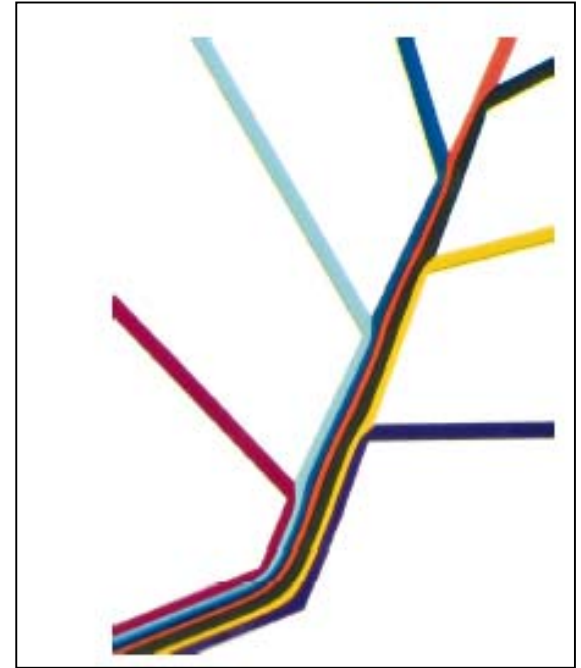
Dimensionless Parameters

- Assume water flow;
 $\mu=10^{-3}$ kg/(s-m), $\rho=10^3$ kg/m³
- Length ~ 10 $\mu\text{m}=10^{-5}$ m
- Velocity ~ 1 mm/s= 10^{-3} m/s
- Then: $\text{Re}=10^{-2}$, $\text{Fr}^2=100$,
- N-S equation becomes Poisson Eqn

$$0 = -\nabla p + \nabla^2 V$$

Re in BioChips and Laminar Flow

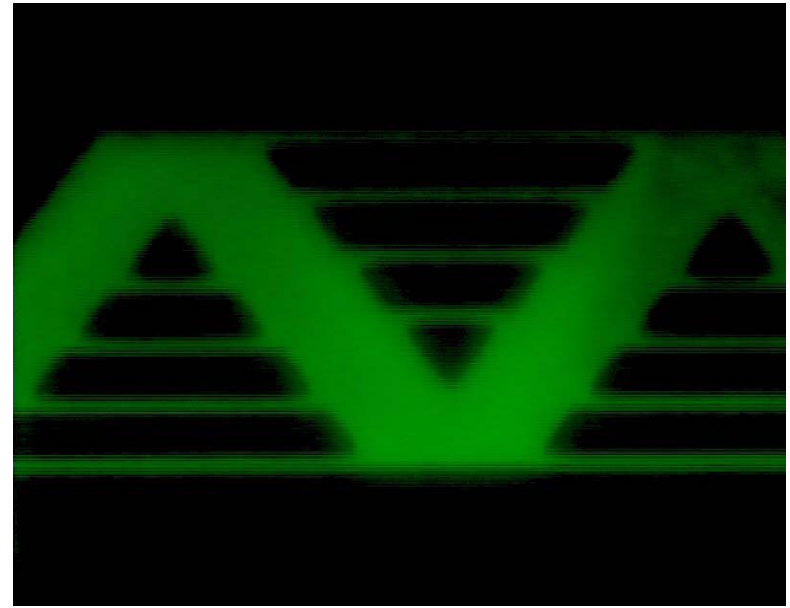
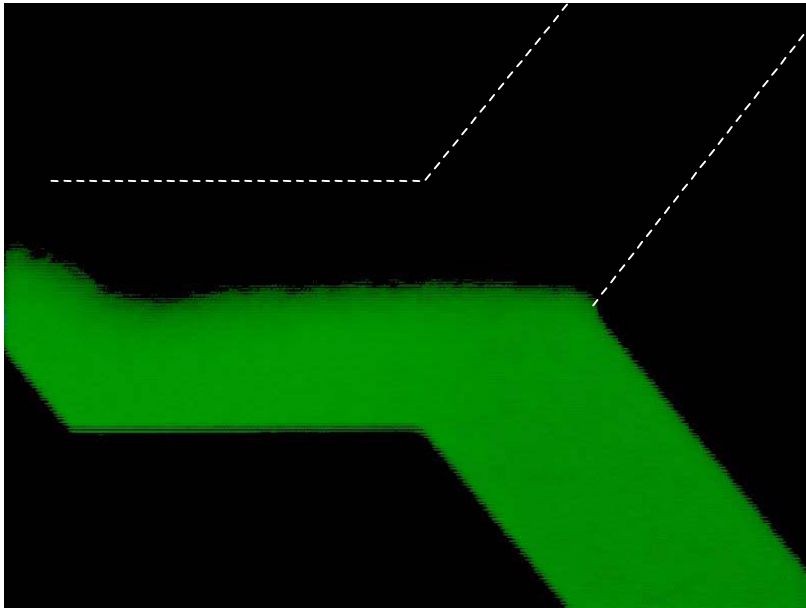
- Reynolds number, $Re = LV_{avg} \rho / \mu$
- $Re = \text{inertial forces} / \text{viscous forces}$ implies inertia relatively important
 - L is the most relevant length scale,
 - μ is the viscosity, ρ is the fluid density,
 - V_{avg} is the average velocity of the flow.
- Reduced Re
 - Higher μ (molasses)
 - Reduce flow rate (traffic in Rome!)
 - Reduce L (i.e. micro devices)
- Re is usually much less than 100, often less than 1.0 in micro devices
- Flow is completely laminar and no turbulence occurs.



Whitesides et al., (Harvard)

Microfluidic Mixing

- Mixing only by diffusion (or novel structures using hydrodynamics)

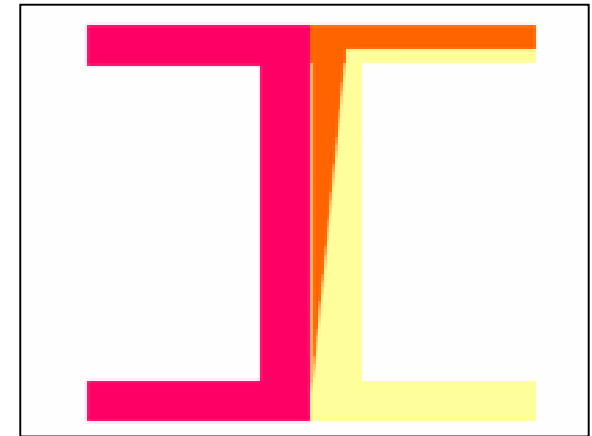


Regnier, et al. Purdue

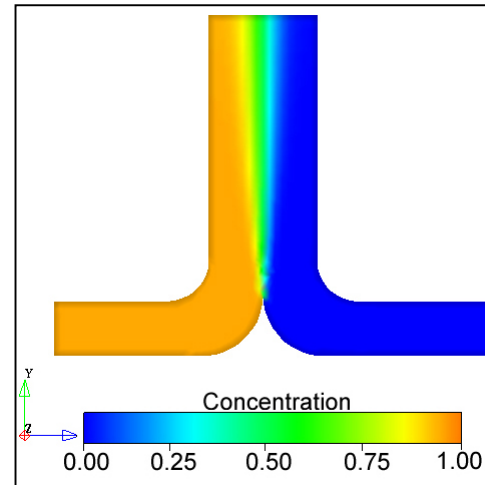
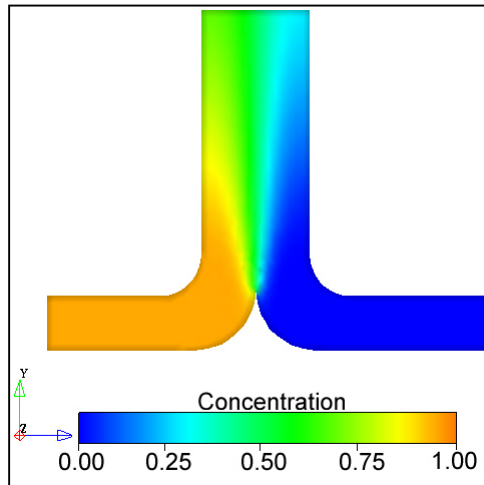
Particle Separation

- Particle separation/filter in micro-fluidic devices - without a membrane
- Smaller particles will diffuse farther and will get separated from the flow
- Diffusion distance: $x^2 = 2Dt$
 - biotin ($D \sim 350 \mu\text{m}^2/\text{s}$)
 - albumin ($D \sim 65 \mu\text{m}^2/\text{s}$)

$$D = \frac{k_b T}{6\pi\eta a}$$

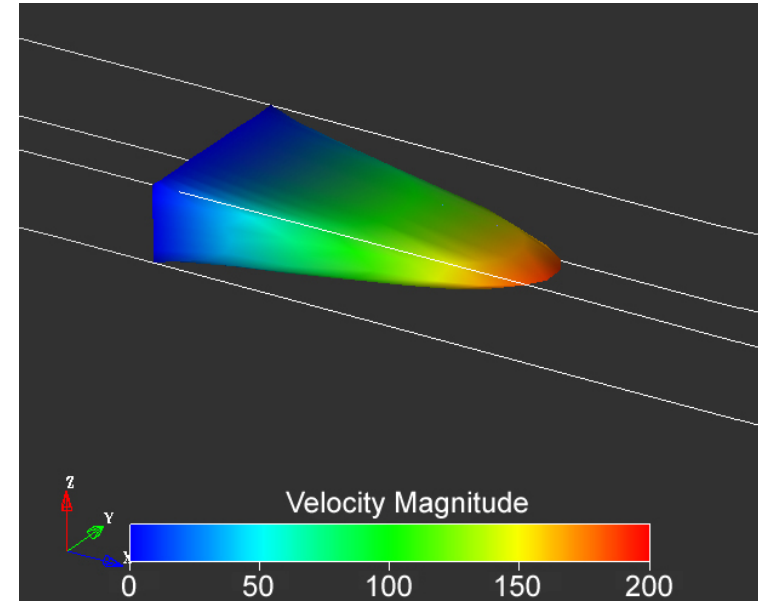


Yager (U. Washington)



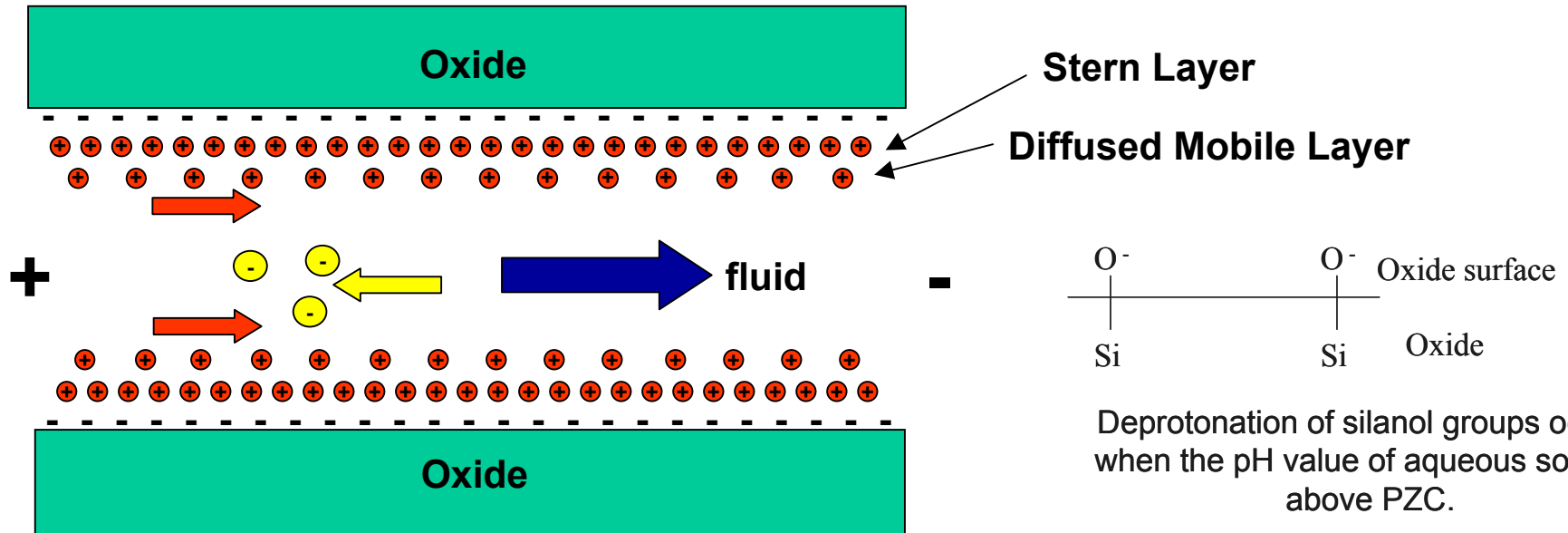
Microfluidic Flow

- Pressure driven flow
 - Parabolic profile
 - No-slip boundary condition (Velocity at interface is zero)
- Electrokinetic flow
 1. Electroosmosis (EOF)
 2. Electrophoresis (EP)
 3. Dielectrophoresis (DEP)



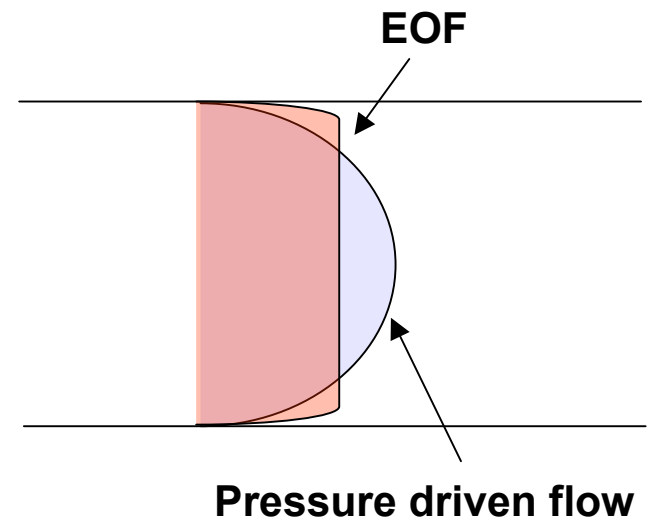
Yager, et al. U. Washington

Electroosmotic Flow

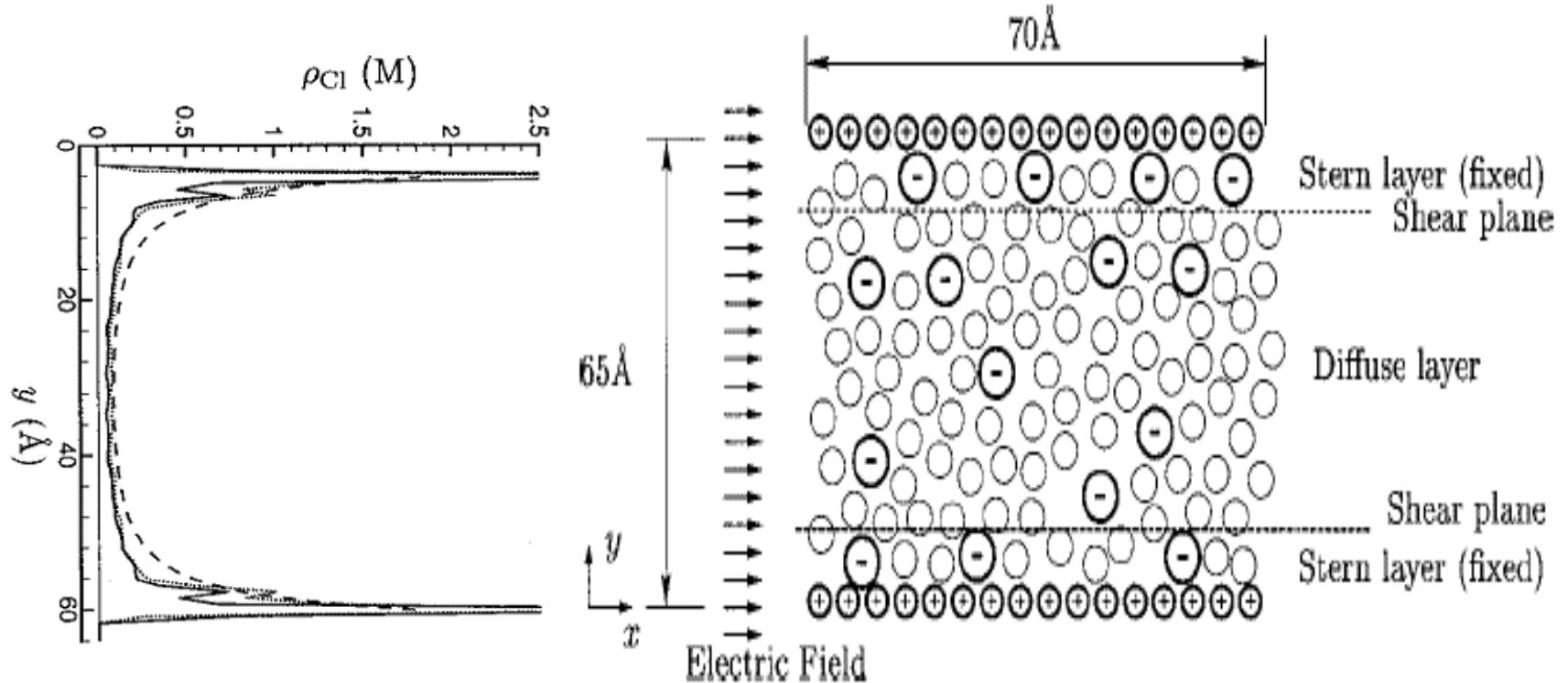


Deprotonation of silanol groups occurs when the pH value of aqueous solution above PZC.

- $Q_{EOF} = \epsilon E \zeta A/\eta$
 ζ = zeta potential, η = viscosity
- Charges at interface
- Counter ion accumulation at interface
- Results in plug flow
- Electrophoresis also takes place

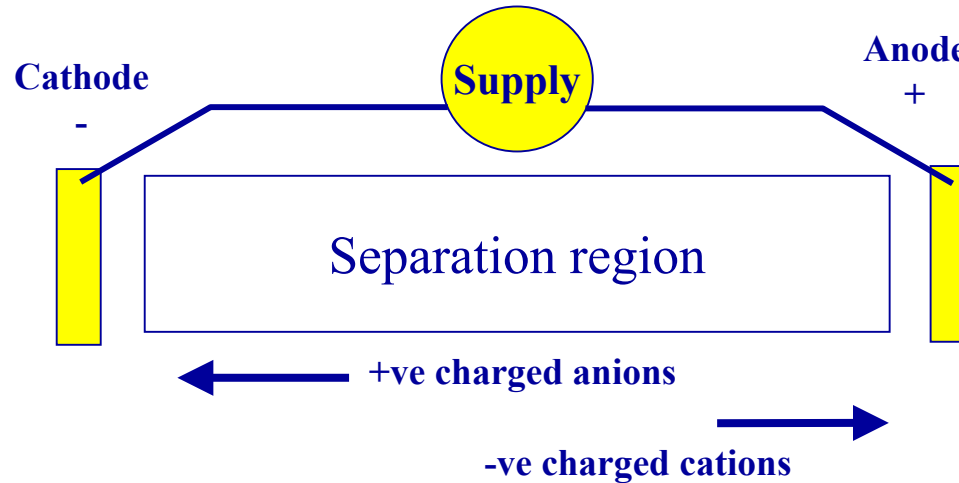


Electroosmotic Flow in Nano-channels



Surface was assumed positively charged. Concentration of Cl ions in bulk is 0.01 M. Concentrations near surface and at middle of channel are 3.21 M and 0.2 M, respectively. ———simulation with uniformly charged wall atoms; ----- simulation with discrete wall atom charges. From *Freund 2002*.

Electrophoresis



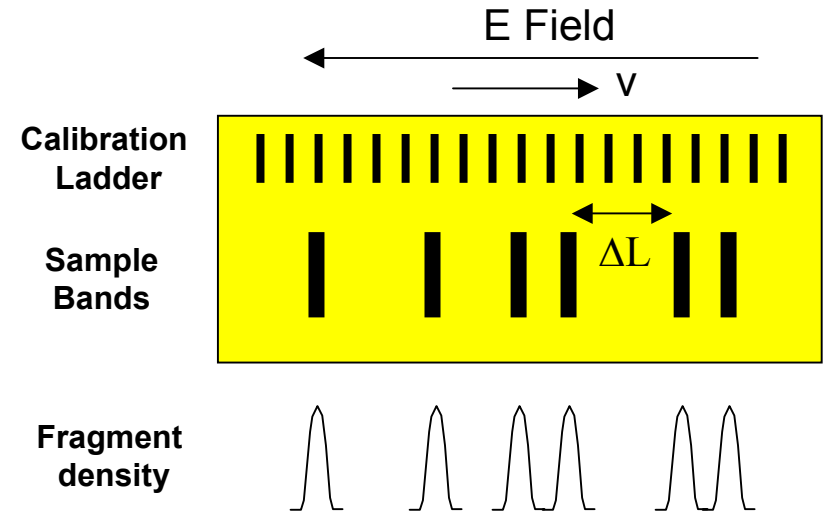
- Electrophoresis: charged species drift when placed under an electric field
- $v = -\mu dV/dx$
 - v - electrophoretic velocity
 - μ - electrophoretic mobility
 - $dV/dx =$ applied electric field

DNA Gel Electrophoresis

- DNA has phosphate backbone which is negatively charged - hence DNA drifts in an E-field
- The charge/mass (e/m) ratio is constant hence electrophoretic mobility is independent of size in liquid medium.
- Thus, another sieving medium is needed where separation can take place due to difference in length.
- The separation region is filled with a gel - sieving matrix with pores through which the DNA molecules can traverse.
- The field stretches the molecules and they move in a snake-like fashion through the pores of the gel.
- μ in gels is inversely proportional to log of fragment size (sieving effect)
- Polyacrylamide gel is used to separate DNA molecules of 10-500 bases - pores are small
- Agarose gel is used to separate larger molecules (300-10,000 base pairs)

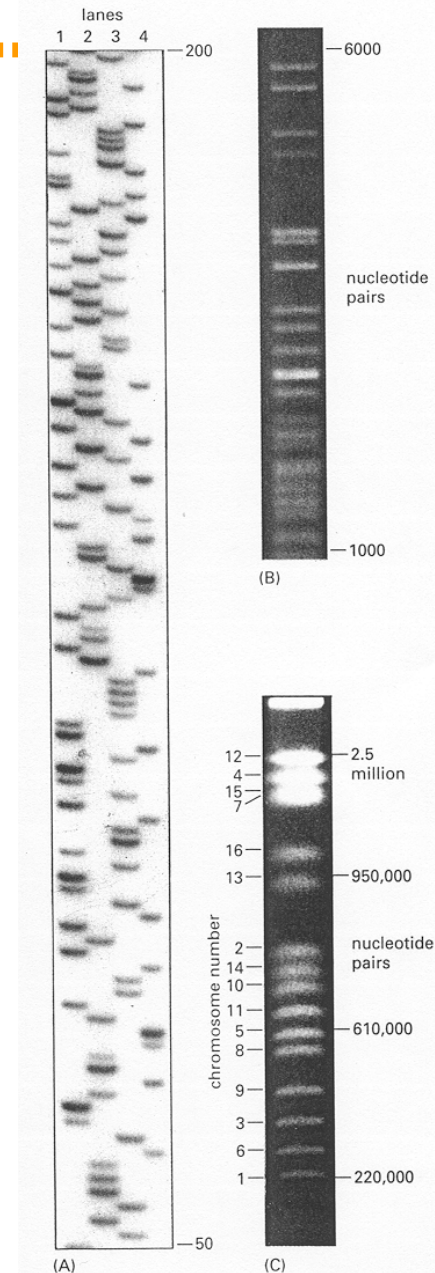
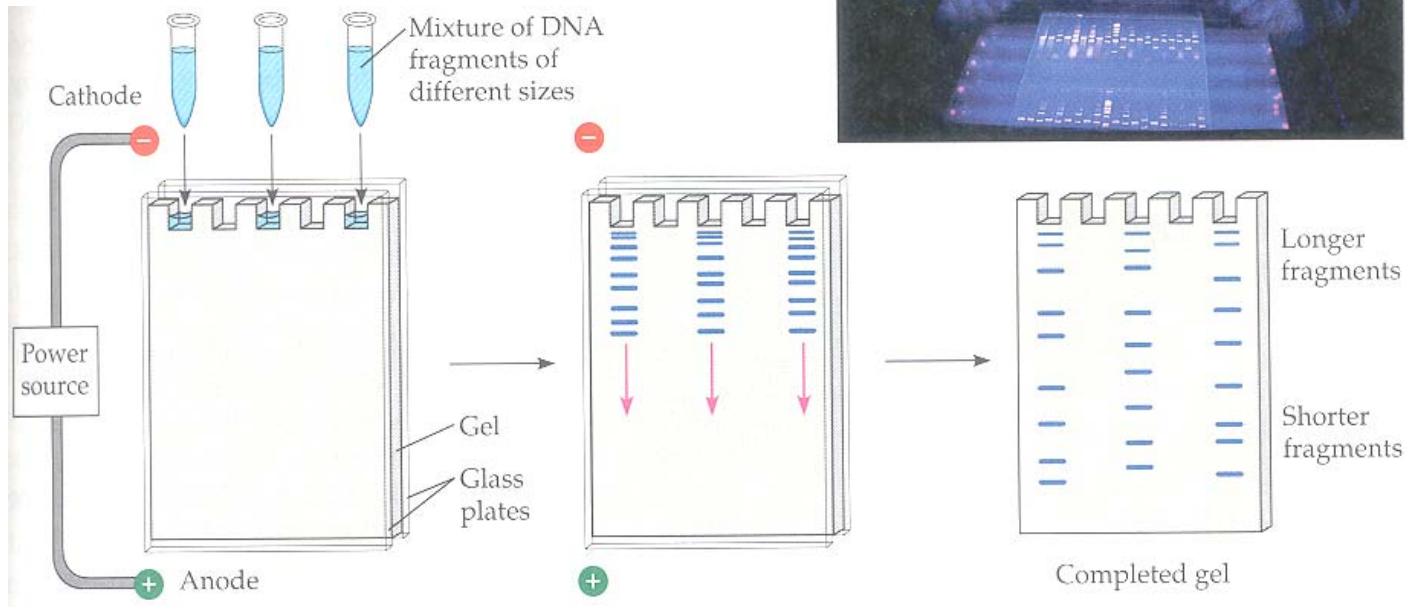
DNA Electrophoresis

- Separation $\Delta L = \Delta\mu E t$
- Resolution of separation is measured by planes N,
 - $N = (\# \text{ of distinguishable bands within the length of the gel})^2$
 - $N = \mu V / 2D$
 - D is the diffusion coefficient

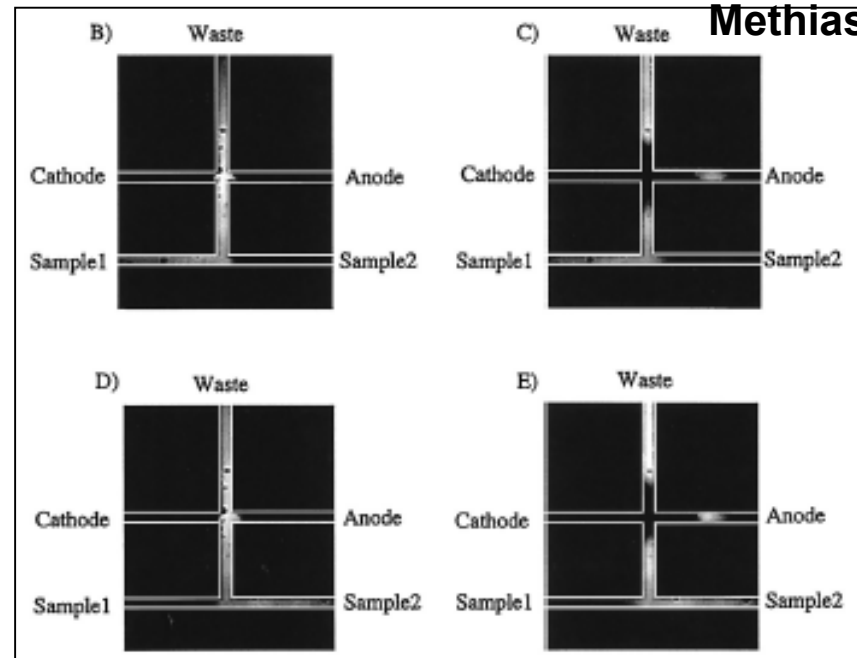
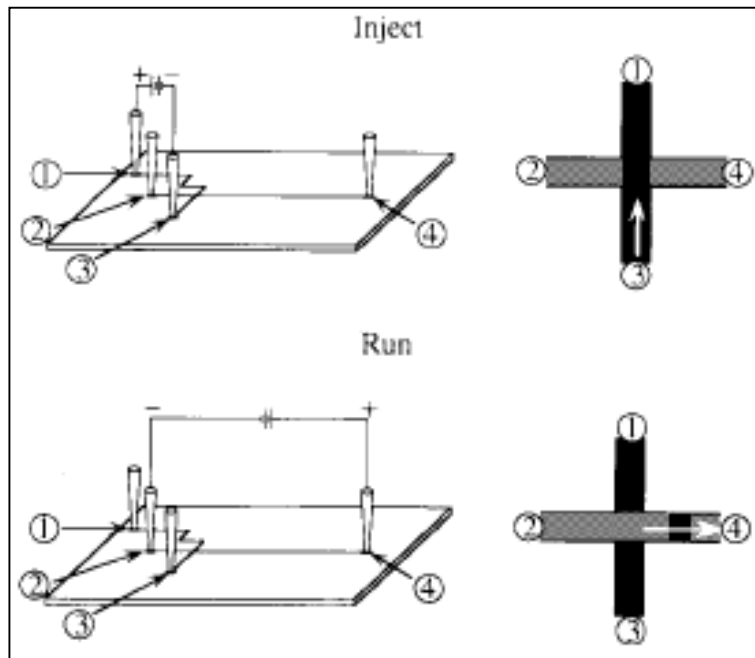


- Higher voltages increase resolution but Joule heating is an issue and needs to be considered
- Separation can also be done in capillaries since higher fields can be used (higher velocities and shorter times)

DNA Electrophoresis



DNA Electrophoresis in a Chip



Methias, UCB

- Small sample size
- Higher fields, higher velocities
- Faster results

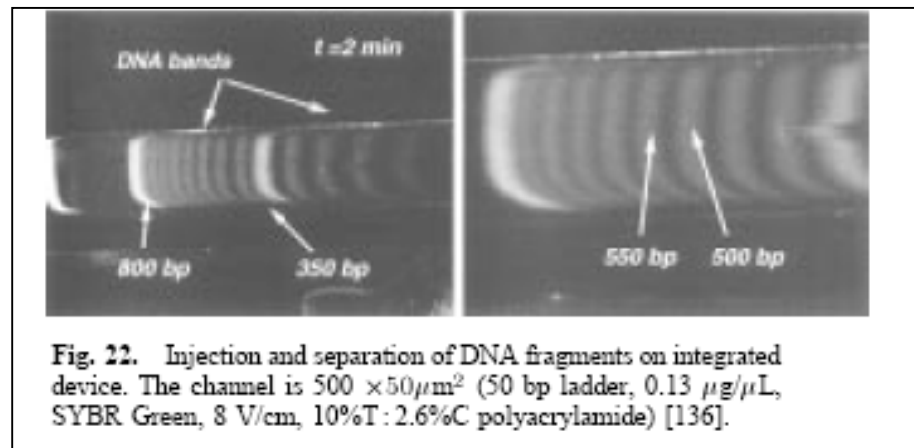
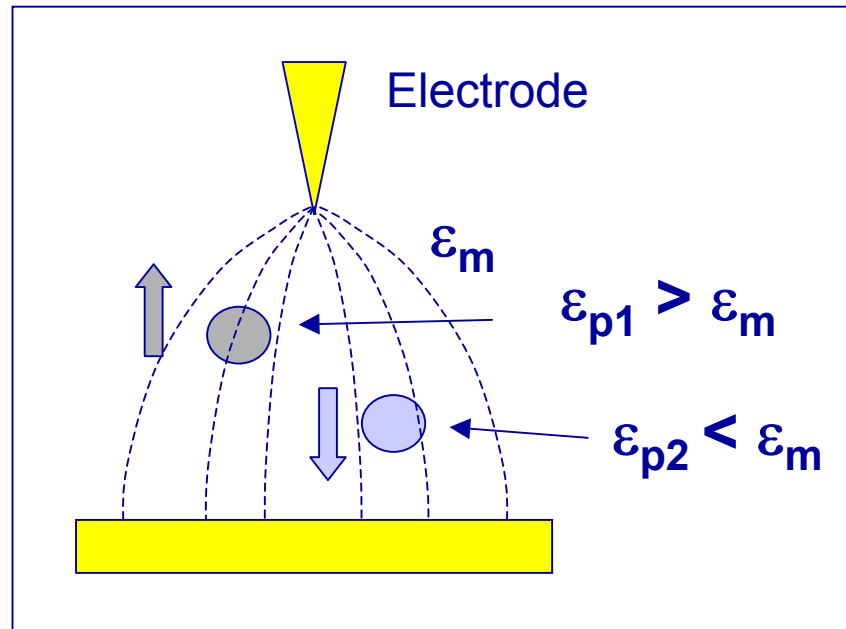


Fig. 22. Injection and separation of DNA fragments on integrated device. The channel is $500 \times 50 \mu\text{m}^2$ (50 bp ladder, $0.13 \mu\text{g}/\mu\text{L}$, SYBR Green, $8 \text{ V}/\text{cm}$, 10%T:2.6%C polyacrylamide) [136].

Dielectrophoresis

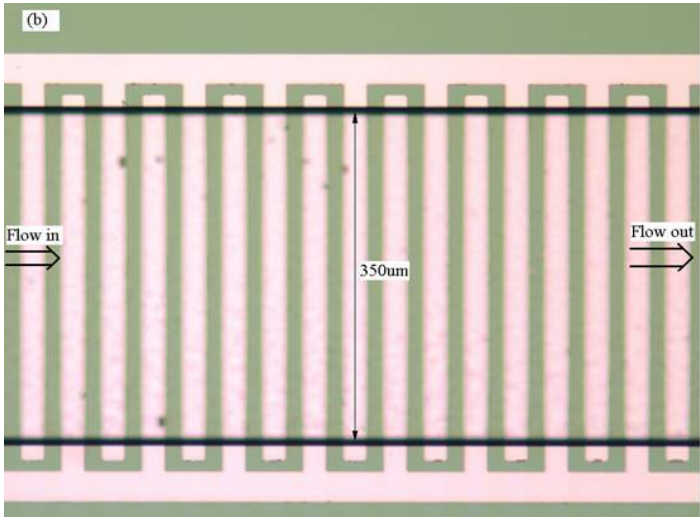


Simplest approximation:

$$F = 2\pi\epsilon_0\epsilon_m r^3 \operatorname{Re}[f_{CM}] \nabla |E_{RMS}|^2$$

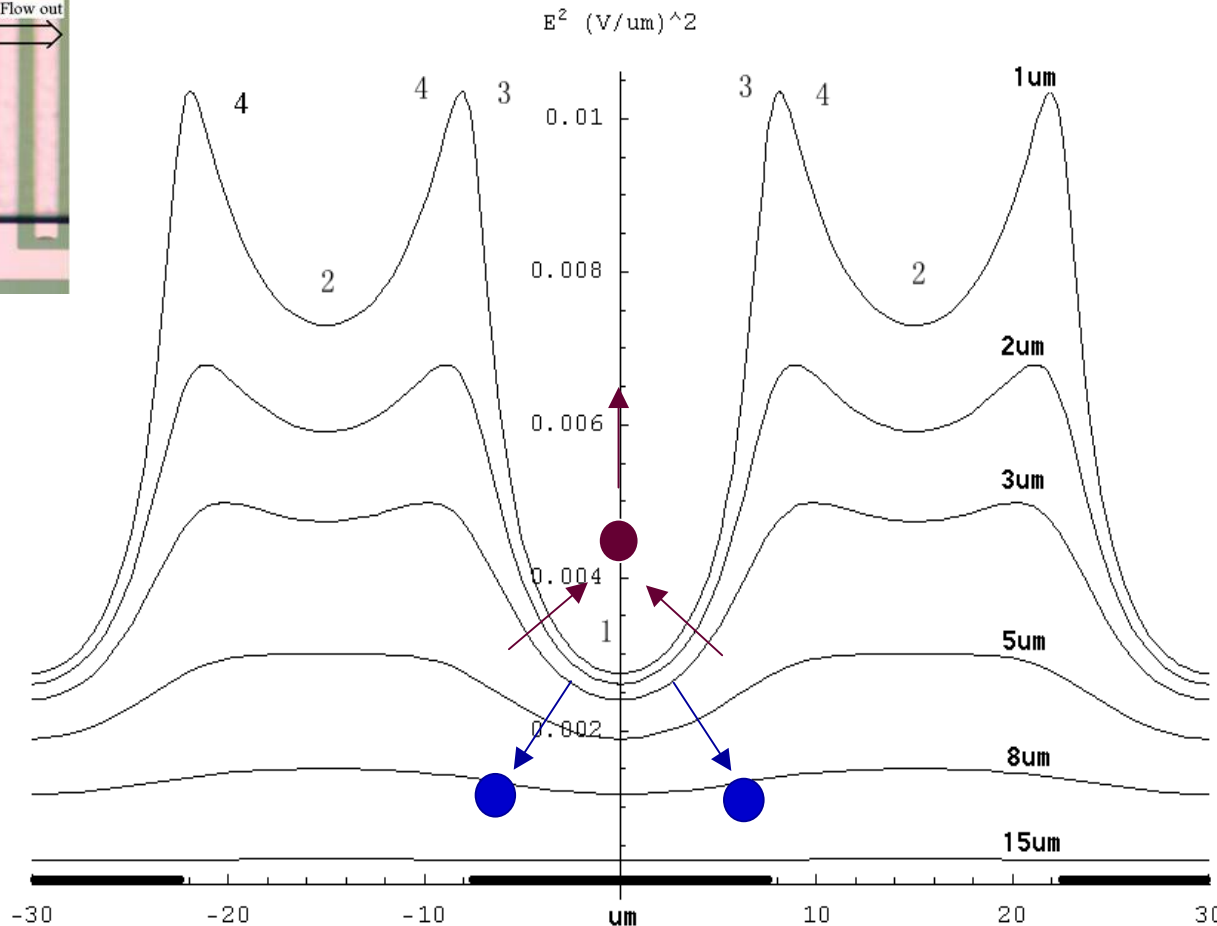
$$f_{CM}(\epsilon_p, \epsilon_m) = \frac{\epsilon_p - \epsilon_m}{\epsilon_p + 2\epsilon_m} \quad \epsilon_p = \epsilon(\omega)$$

Dielectrophoresis on Interdigitated Electrodes

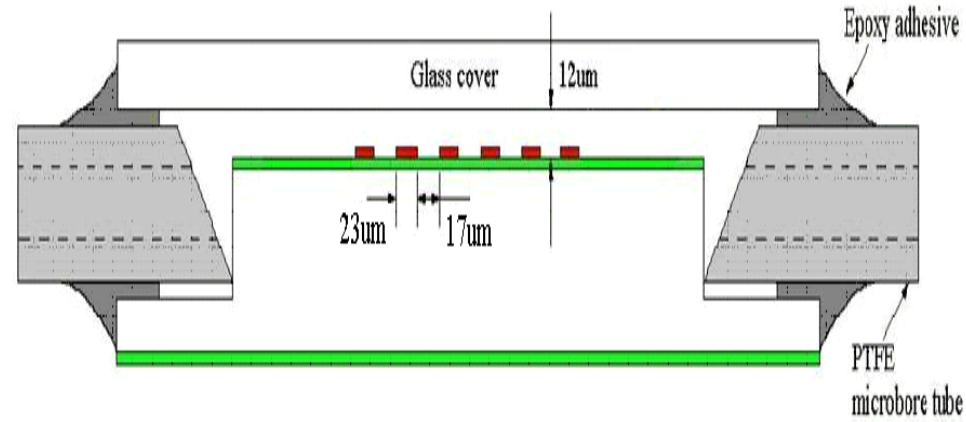
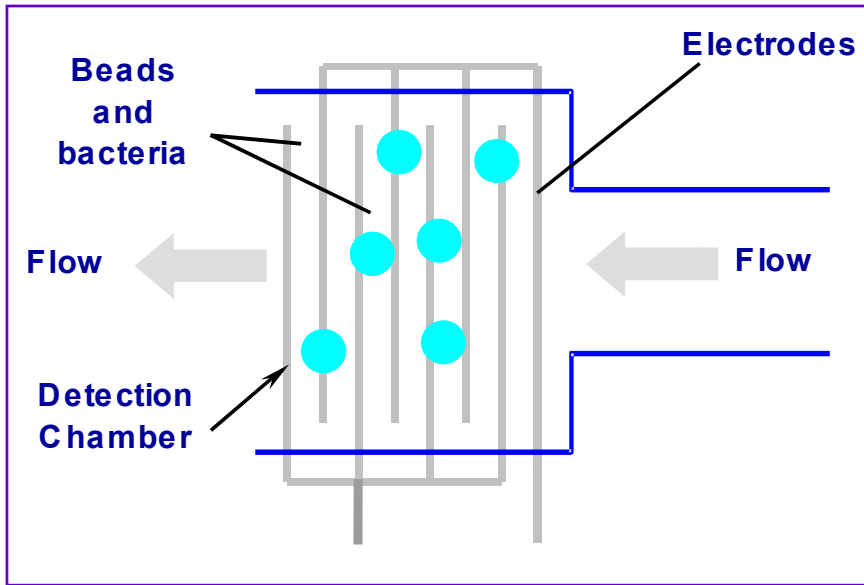


Interdigitated electrodes on a chip

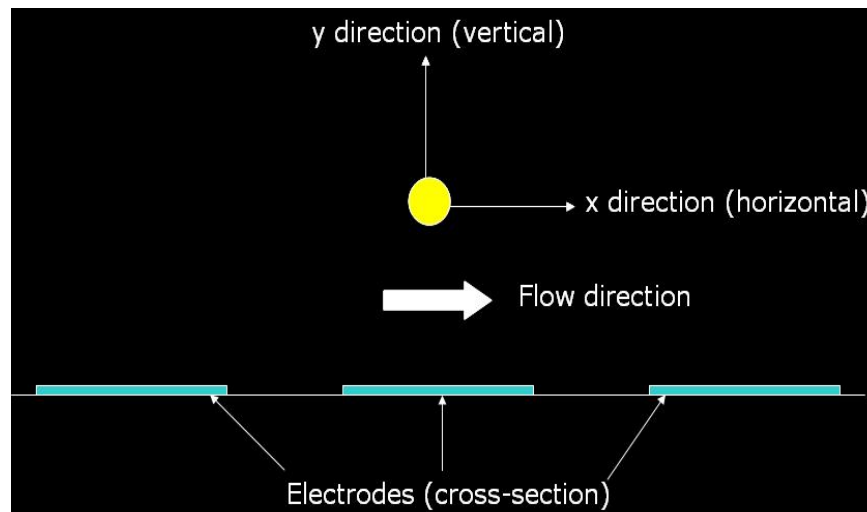
Polystyrene beads : $\epsilon_p < \epsilon_m \rightarrow$ negative DEP
 Cells : $\epsilon_p < \epsilon_m \rightarrow$ Negative DEP
 Cells : $\epsilon_p > \epsilon_m \rightarrow$ Positive DEP



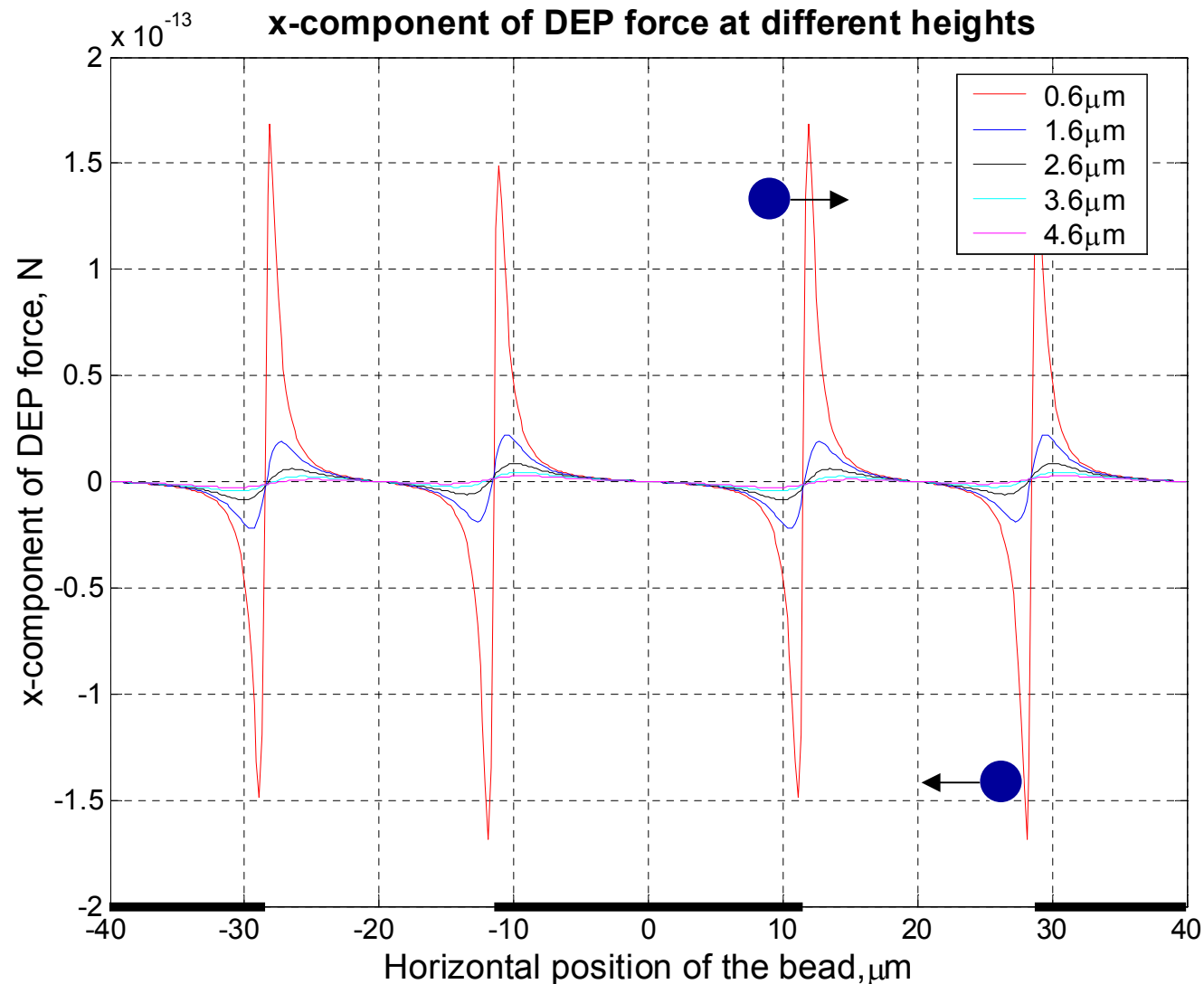
A Dielectrophoretic Filter



Schematic of the device cross-section

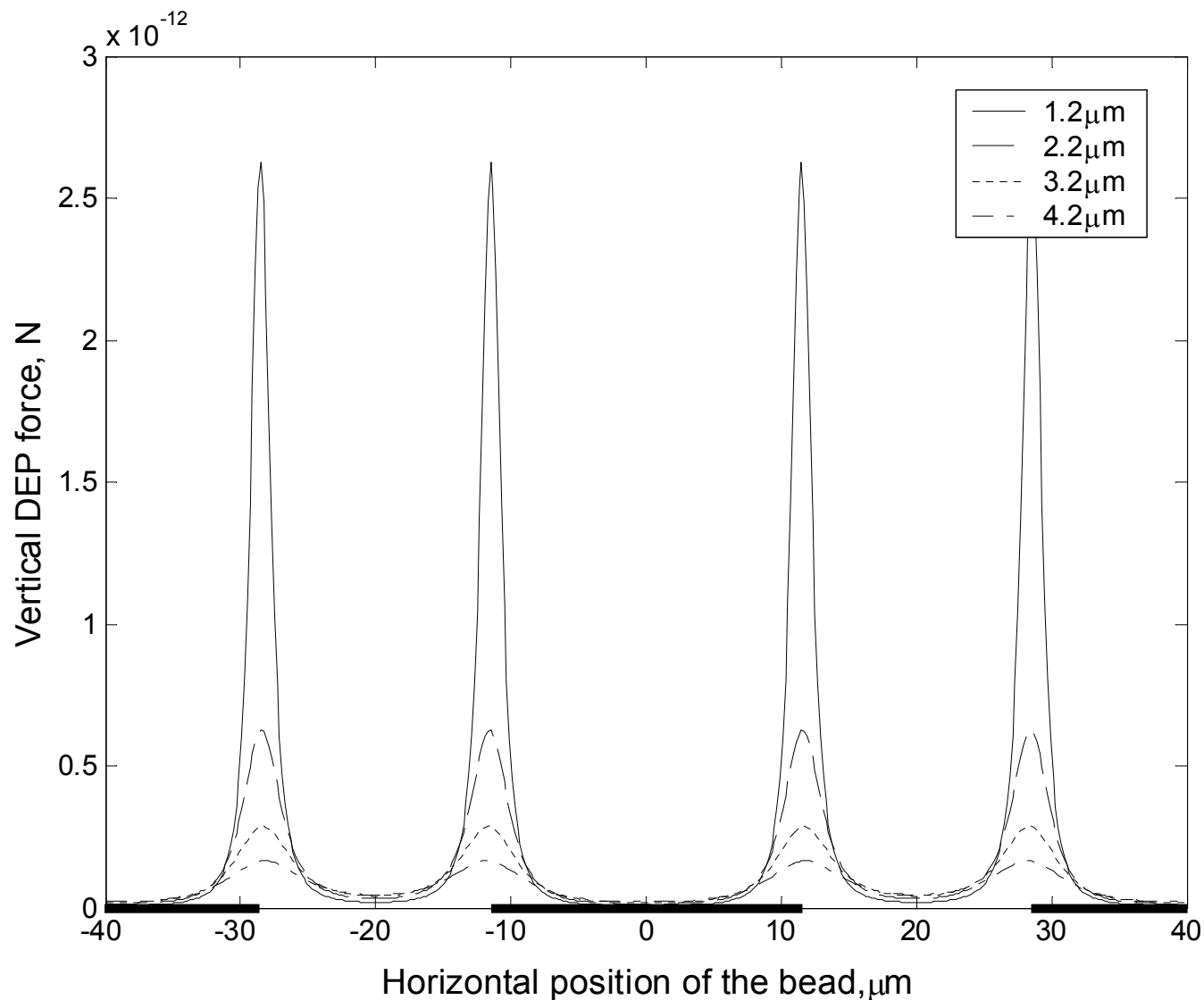


X-component of DEP force at different heights



- **Bead diameter:** 0.7 μm
- **Bead conductivity:** 2e-4 S/m
- **Relative permittivity of bead:** 2.6
- **Bead density:** 1.05 g/cm³
- **Medium (DI water) conductivity:** 2.5 S/m
- **Relative permittivity of medium:** 80
- **Medium density:** 1.0 g/cm³
- **Voltage:** 1Vrms
- **Frequency:** 580KHz ¹⁸

Y-component of DEP force at different heights



Forces on a particle in a micro-fluidic flow

- 1. DEP Force
- 2. Sedimentation Force

$$F_{sedi} = \frac{4}{3} \pi R^3 (\rho_p - \rho_m) g$$

- 3. Hydrodynamic Drag Force:

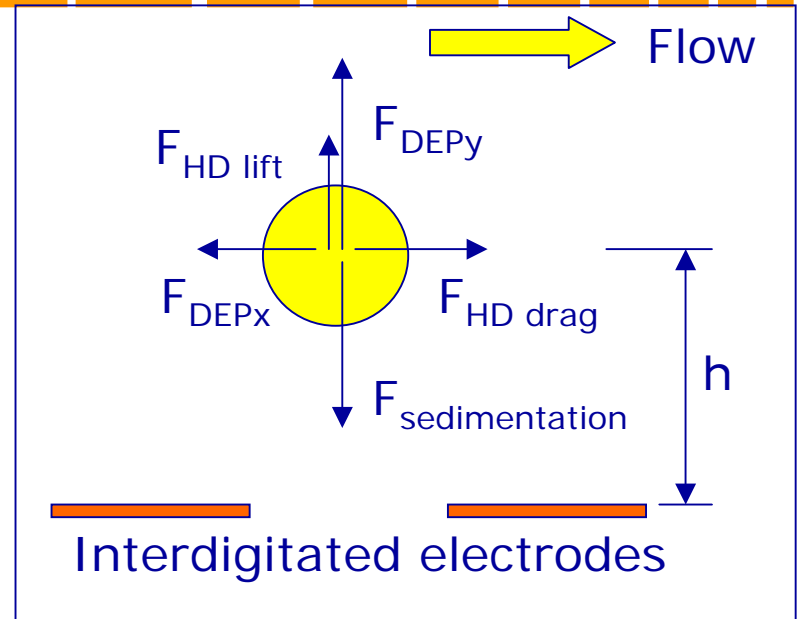
$$F_{HD-drag} \approx 6\pi kR \eta (v_m - v_p)$$

- Assume a parabolic laminar flow profile:

$$v = 6 \langle v \rangle \frac{x}{h} \left(1 - \frac{x}{h} \right) \quad \langle v \rangle = \frac{U}{wh}$$

- 4. Hydrodynamic lifting force

$$F_{HD-lift} \approx 0.153 R^2 \eta \frac{1}{(x-R)} \cdot \frac{dv_m}{dx} \Big|_{x=0}$$

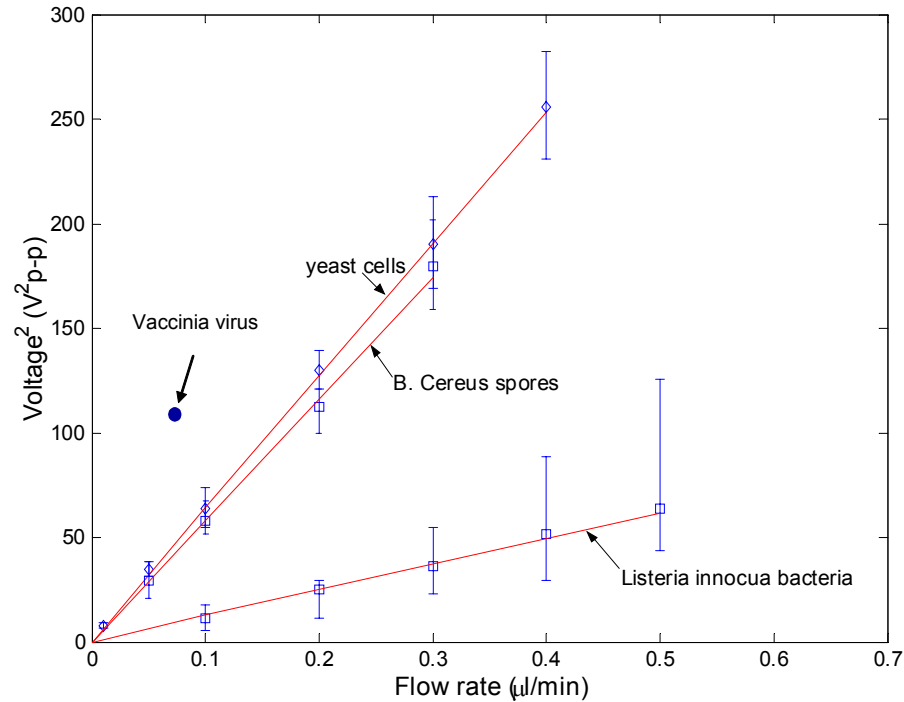
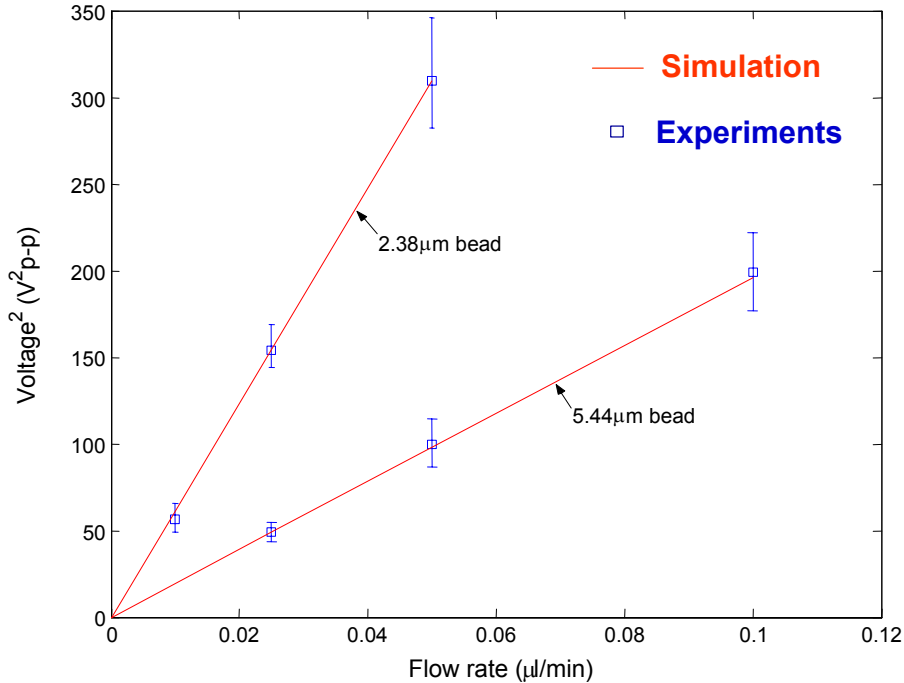


U: flow rate in $\mu\text{l}/\text{min}$

- Two orders of magnitude smaller than typical DEP lifting force
- Neglected here

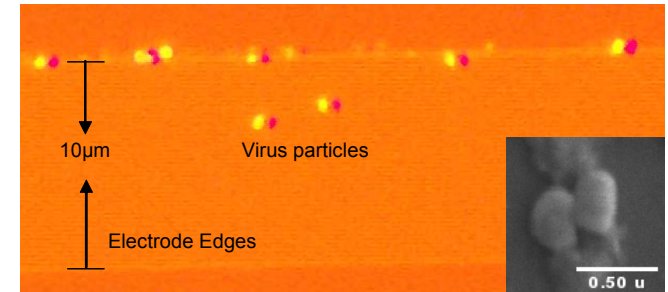
Trapping of beads (- DEP) and microorganisms (+ DEP)

Holding voltage of the negative DEP traps on interdigitated electrodes versus flow rate for polystyrene beads with different diameters in DI water (conductivity $\sim 1.5 \mu\text{S}/\text{cm}$) at 1MHz

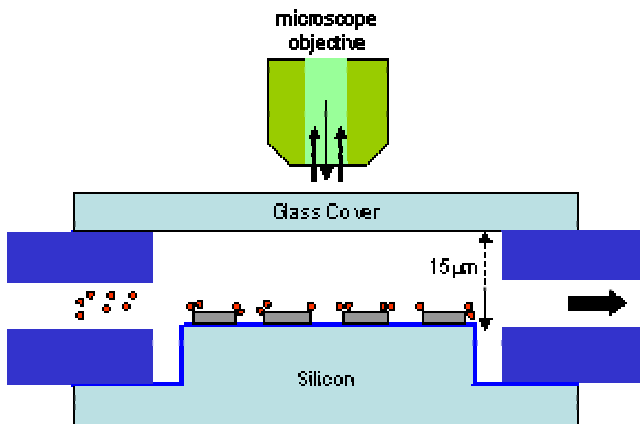


Dielectrophoretic Trapping of *Vaccinia* virus (positive DEP)

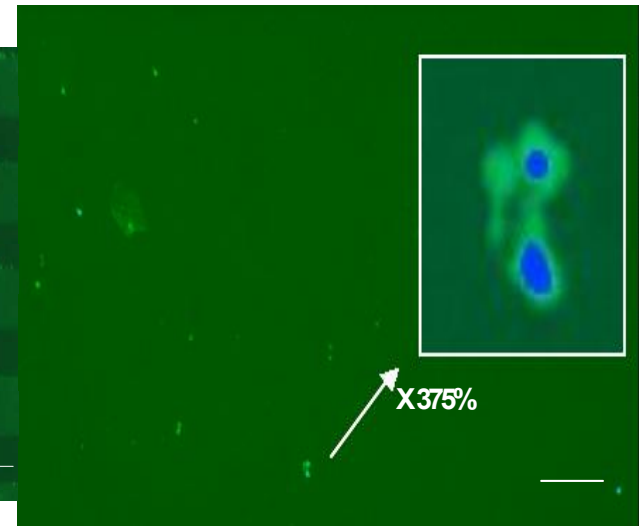
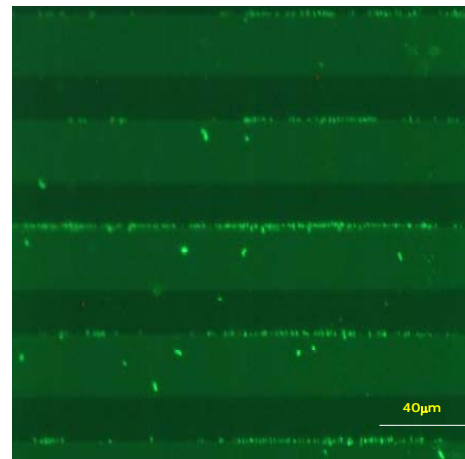
- Fluorescent imaging of nano-scale virus particles (*Vaccinia* virus and Human Corona Virus)
- Trapping of viruses in DEP filters
- Dual labeling of viruses with fluorescent dyes



The dual (DiOC63, green and DiI, red) labelled viral particles



Virus Size ~ 250x350nm
Picture taken at: 10Vpp, 1MHz, DI water
~1.5µS/cm, flow rate ~0.1µl/min



400x magnification: viral surface lipid membrane labeled green (DiOC63) and viral nucleic acids were stained blue (Hoechst 33342 stain)

Release voltage vs. diameter for particle collecting the electrode edge, considering the Brownian motion

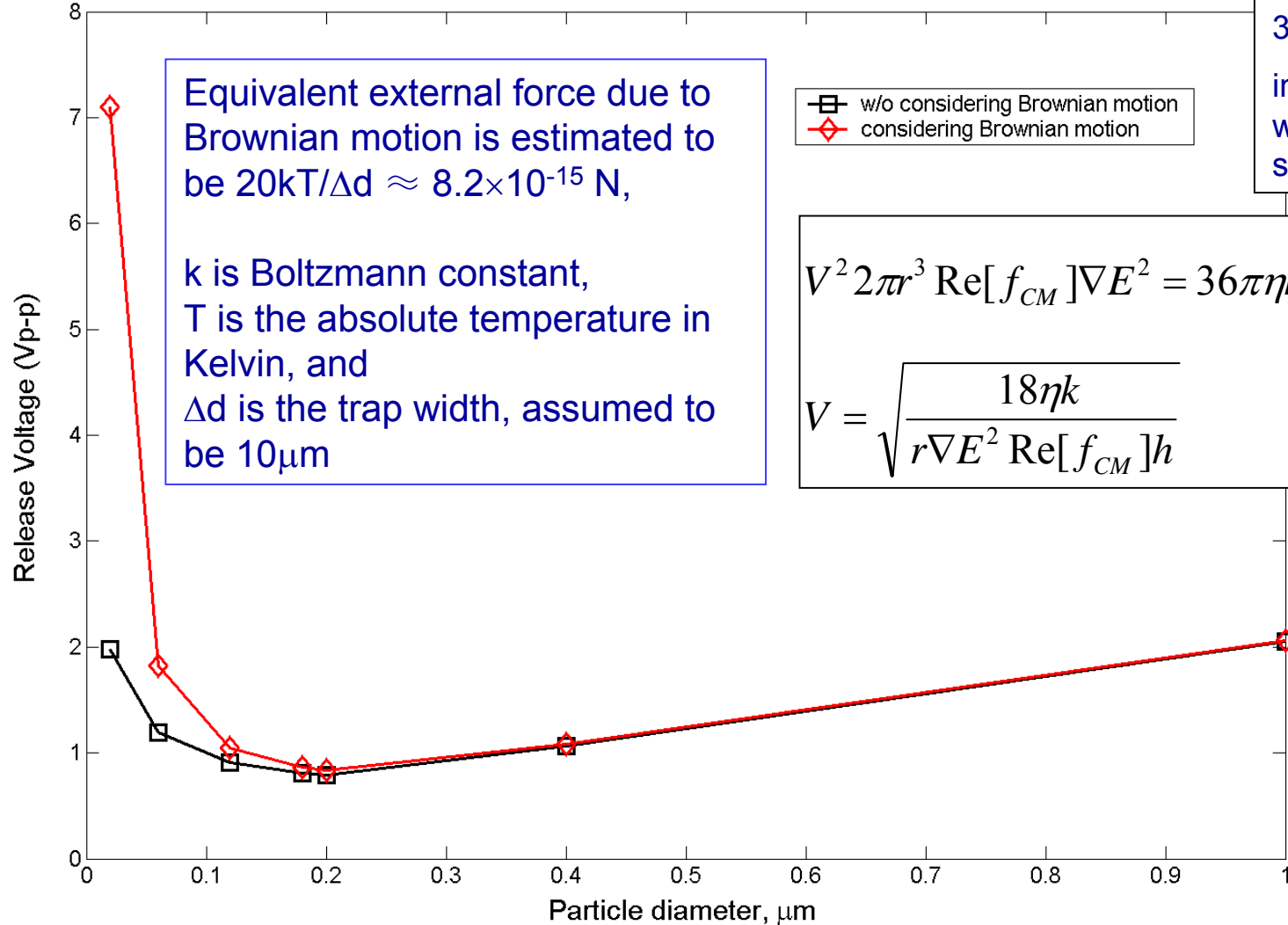
Polarization factor=0.5,
 flow rate 0.1 μm/min, in the channel with cross-section 350x11.6 μm²,
 interdigitated electrodes with 23 μm width and 17 μm spacing

Equivalent external force due to Brownian motion is estimated to be $20kT/\Delta d \approx 8.2 \times 10^{-15}$ N,
 k is Boltzmann constant,
 T is the absolute temperature in Kelvin, and
 Δd is the trap width, assumed to be 10 μm

□ w/o considering Brownian motion
 ◇ considering Brownian motion

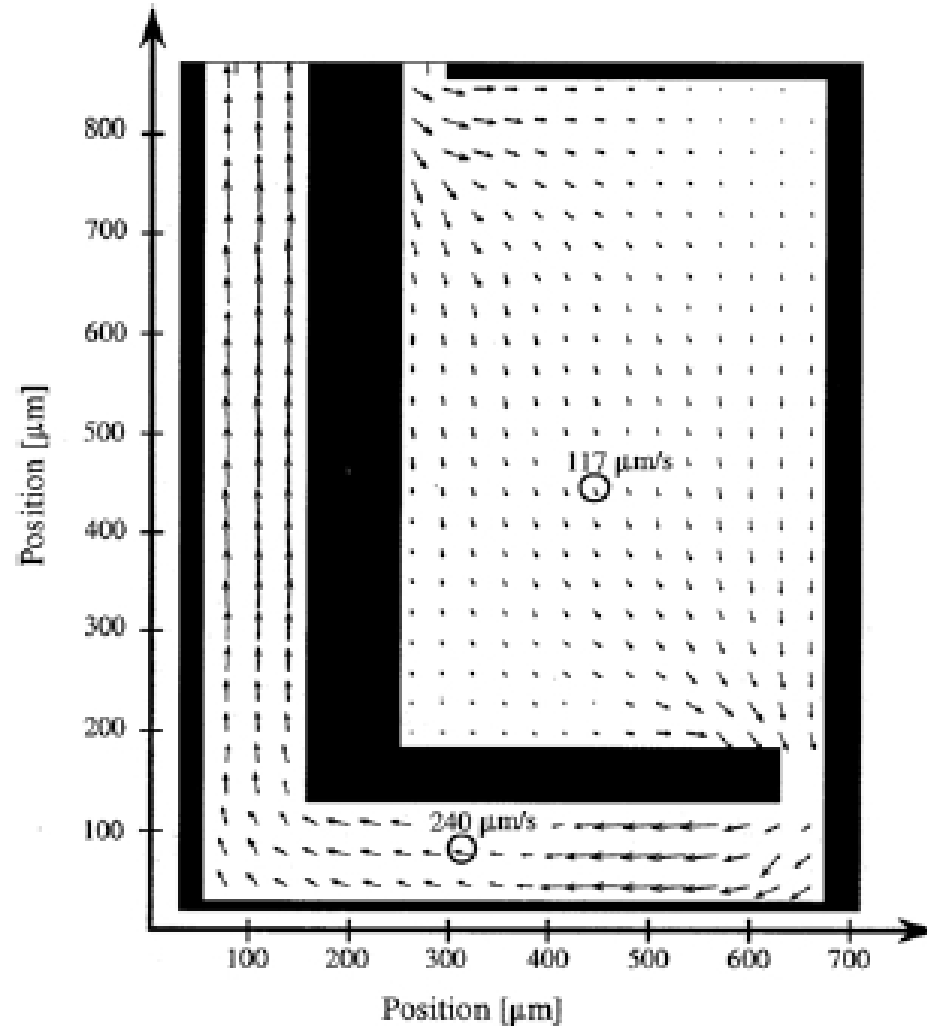
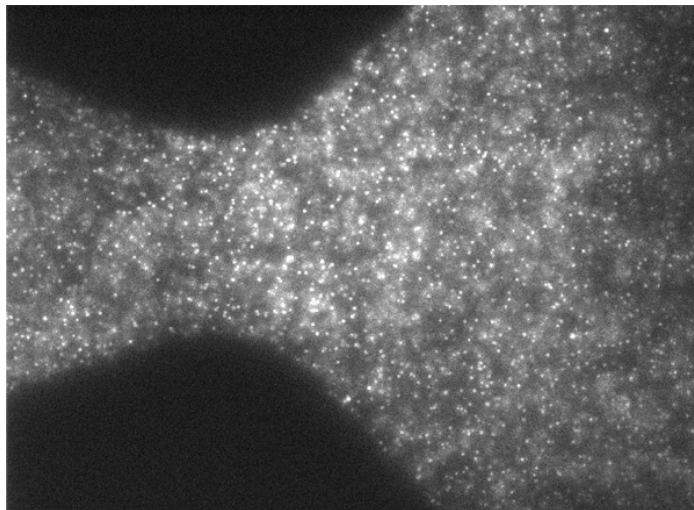
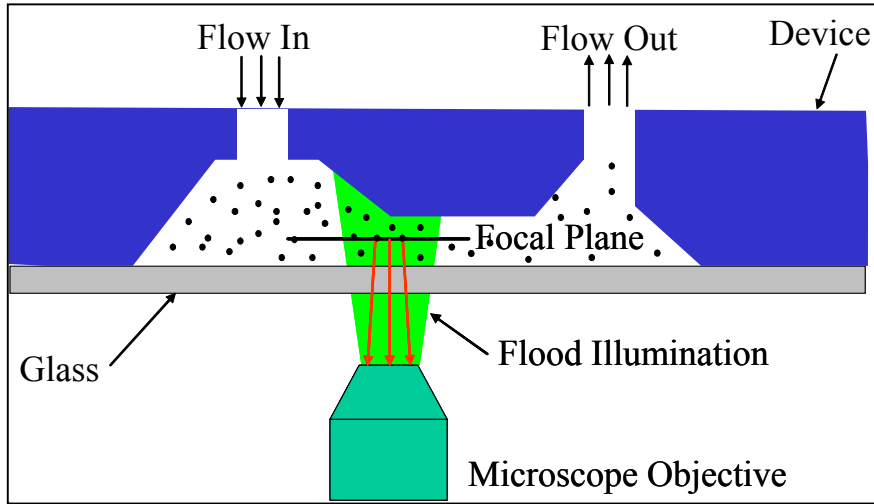
$$V^2 2\pi r^3 \text{Re}[f_{CM}] \nabla E^2 = 36\pi\eta k r \left(\frac{r}{h} - \frac{r^2}{h^2} \right) \approx 36\pi\eta k \frac{r^2}{h}$$

$$V = \sqrt{\frac{18\eta k}{r \nabla E^2 \text{Re}[f_{CM}] h}}$$



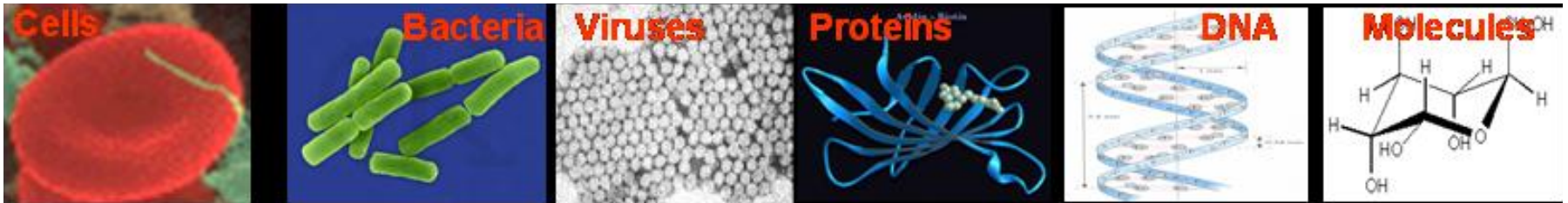
Micro-fluidic Characterization

- Micro-Particle Imaging Velocimetry (μ PIV)



Key Topics

- Biochips/Biosensors and Device Fabrication
- Cells, DNA, Proteins
- Micro-fluidics
- **Biochip Sensors & Detection Methods**
- Micro-arrays
- Lab-on-a-chip Devices



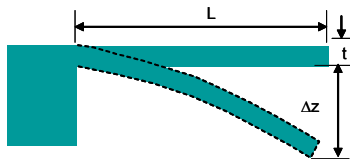
Biochip Sensors

- Detect cells (mammalian, plant, etc.), microorganisms (bacteria, etc.), viruses, proteins, DNA, small molecules
- Use optical, electrical, mechanical approaches at the micro and nanoscale in biochip sensors

Sensing Methods in BioChips

Mechanical Detection

Surface Stress Change Detection



$$\Delta z = 4 \left(\frac{L}{t} \right)^2 \frac{(1-\nu)}{E} (\Delta\sigma_1 - \Delta\sigma_2)$$

- Δz = deflection of the free end of the cantilever
- L = cantilever length
- t = cantilever thickness
- E = Young's modulus
- ν = poisson's ratio
- $\Delta\sigma_1$ change in surface stress on top surface
- $\Delta\sigma_2$ change in surface stress on bottom surface

Mass Change Detection



$$f = \frac{1}{2\pi} \sqrt{\frac{k}{m}}$$

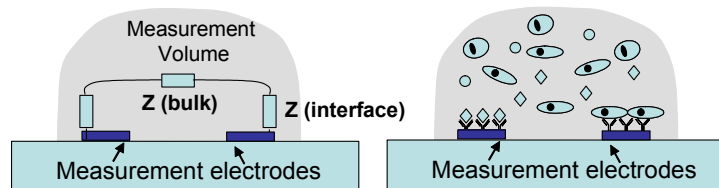
$$\Delta m = \frac{k}{4\pi^2} \left(\frac{1}{f_1^2} - \frac{1}{f_o^2} \right)$$

- k = spring constant
- m = mass of cantilever
- f_o = unloaded resonant frequency
- f_i = loaded resonant frequency

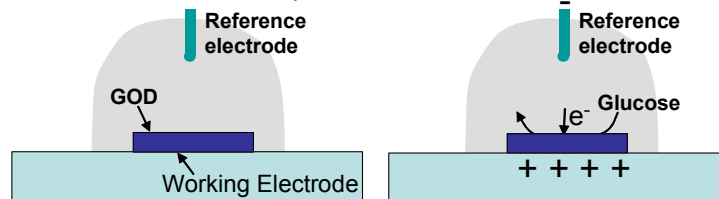
(a)

Electrical Detection

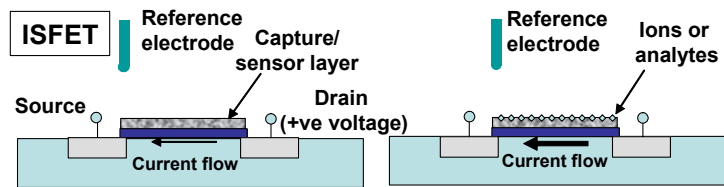
Conductometric Detection



Amperometer Detection

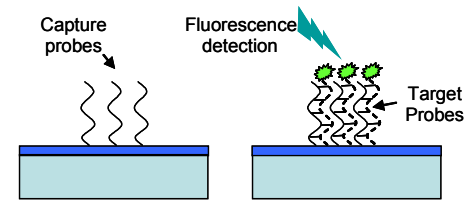


Potentiometric Detection

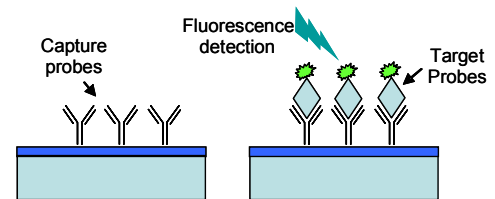


(b)

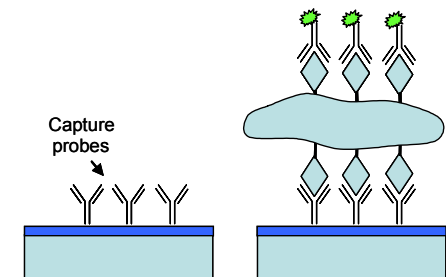
Optical Detection



DNA detection on chip surfaces



Protein detection on chip surfaces



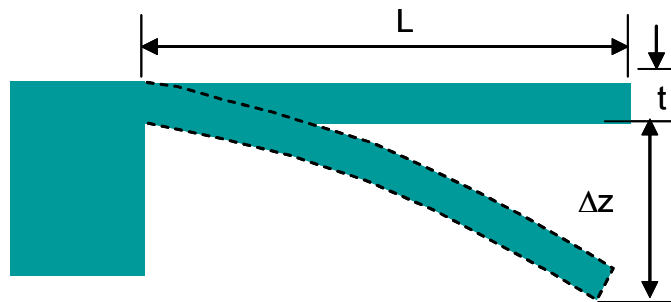
Cell detection on chip surfaces

(c)

1. Microcantilever Stress Sensors

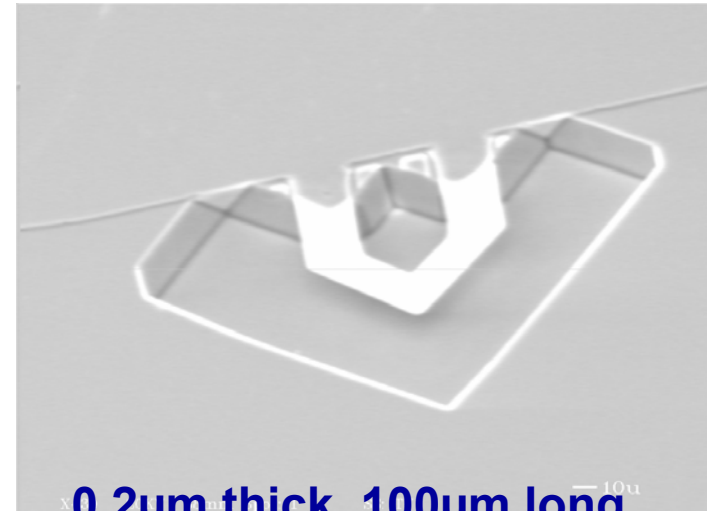
Mechanical Detection

Surface Stress Change Detection



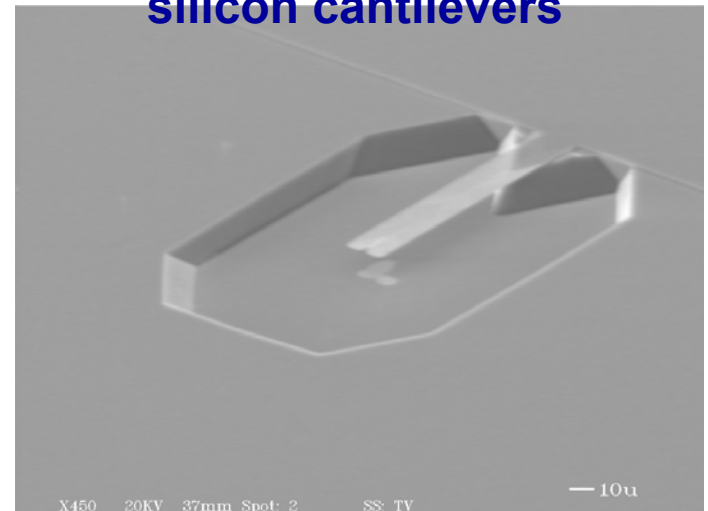
$$\Delta z = 4 \left(\frac{l}{t} \right)^2 \frac{(1-\nu)}{E} (\Delta\sigma_1 - \Delta\sigma_2)$$

- Δz = deflection of the free end of the cantilever
- L = cantilever length
- t = cantilever thickness
- E = Young's modulus
- ν = poisson's ratio
- $\Delta\sigma_1$ change in surface stress on top surface
- $\Delta\sigma_2$ change in surface stress on bottom surface



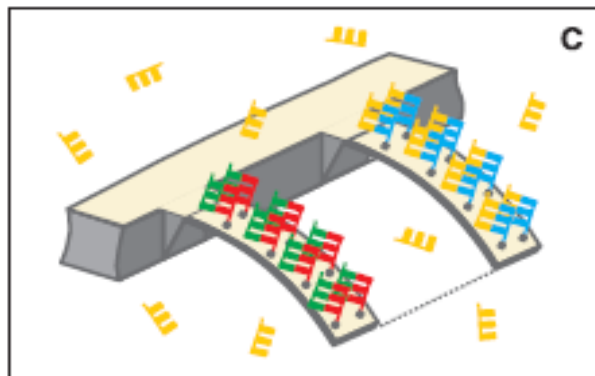
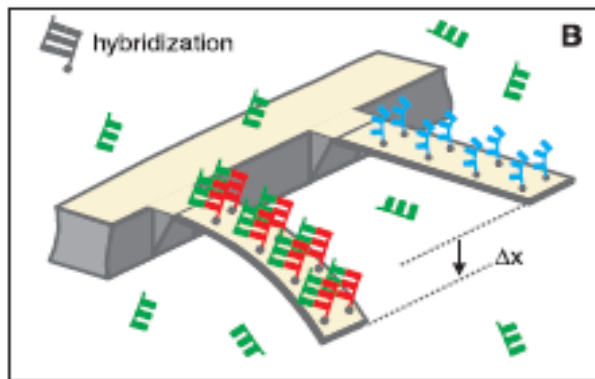
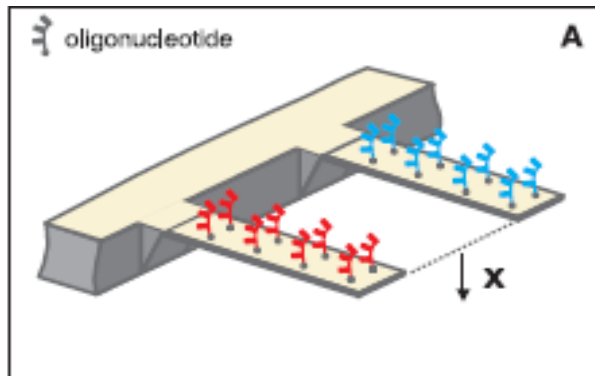
**0.2 μ m thick, 100 μ m long,
silicon cantilevers**

Title: released after ox etch
Comment:
Date: 07-14-2000 Time: 18:28
Filename: 148.TIF

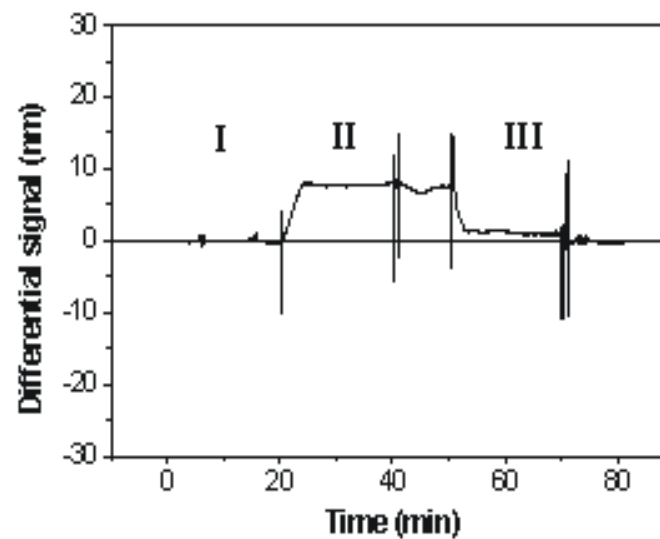
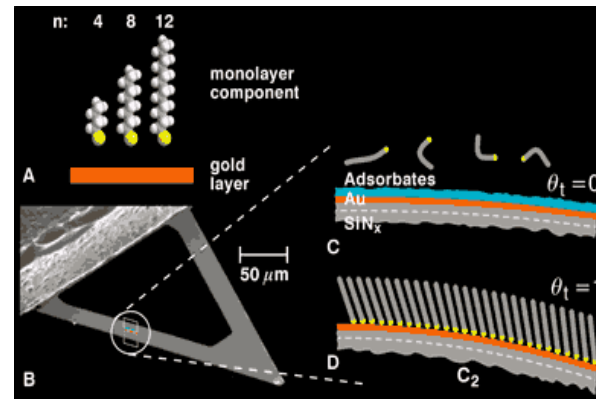


X450 20KV 37mm Spot: 2 SS: TV
Title: released after ox etch
Comment:
Date: 07-14-2000 Time: 18:38
Filename: 150.TIF

Microcantilever Stress Sensors



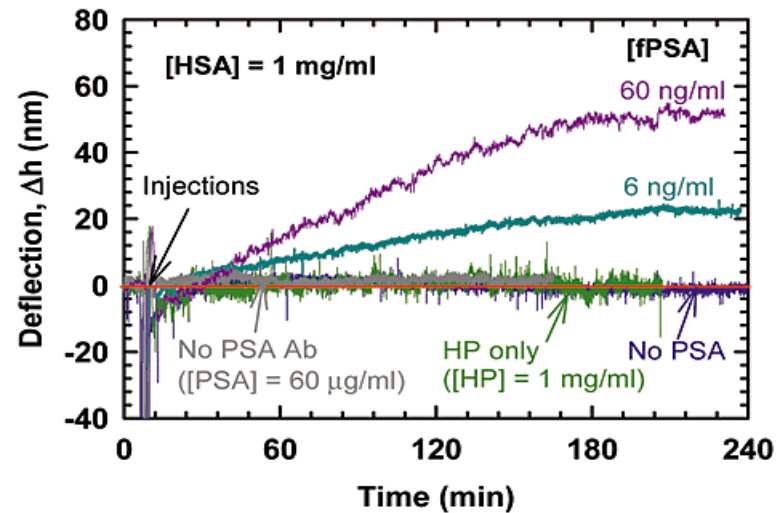
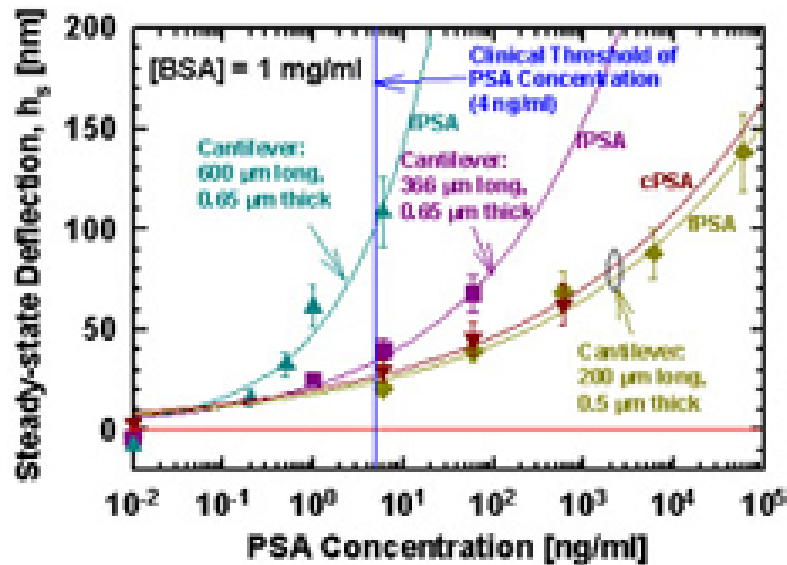
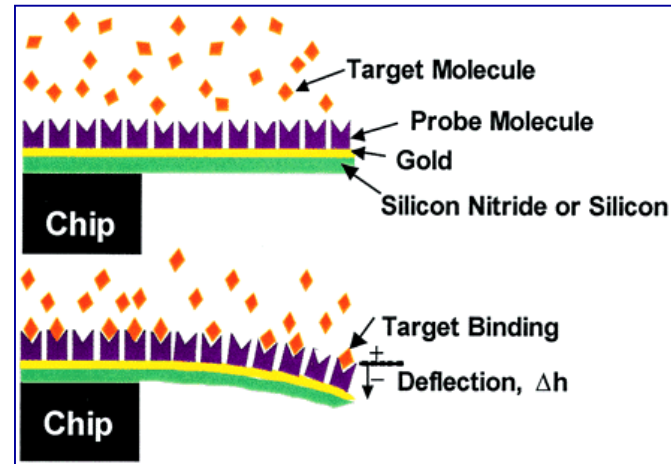
IBM Zurich Research: DNA Detection



Fritz et al, *Science*, **288**, April 2000

Microcantilever Stress Sensors

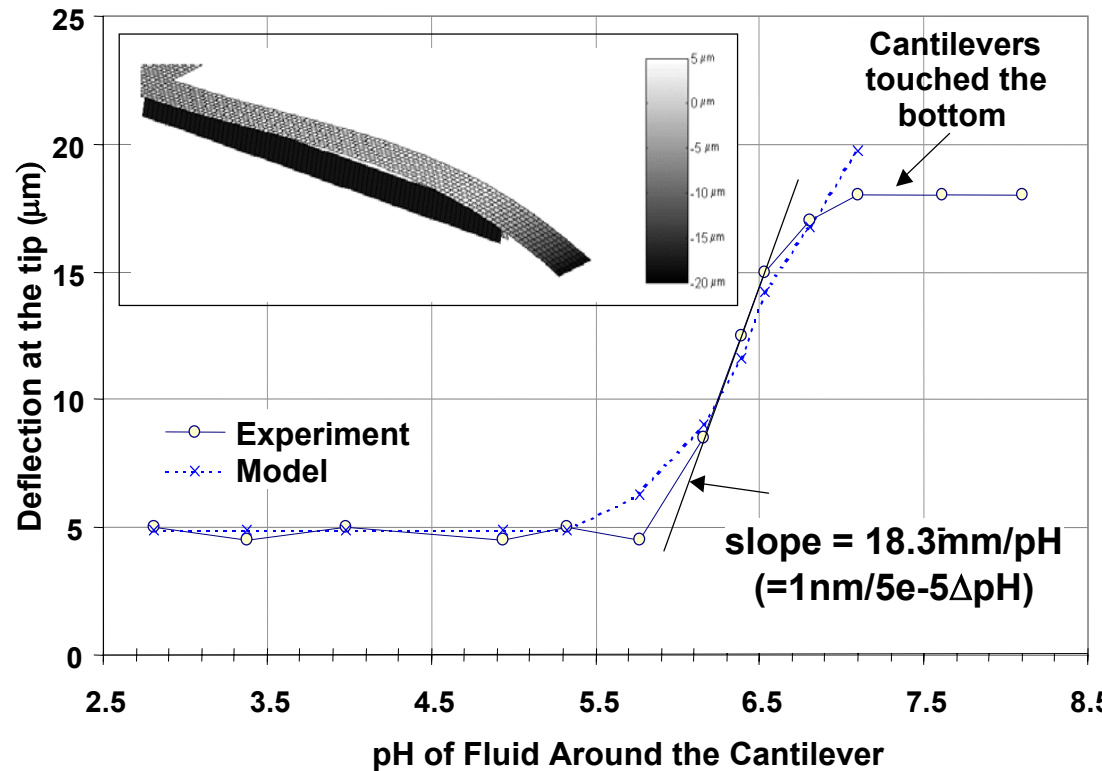
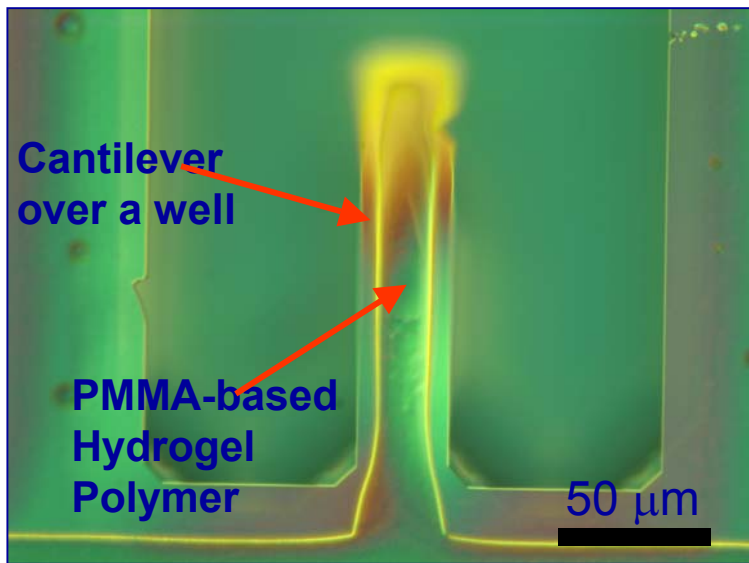
Detection of PSA, Prostate Specific Antigen (cancer marker protein in blood)



- PSA ~ 30kDa ~ $30 \times 1e3 \times 1.66e-24\text{gm}$
- In 1ng/ml ~ $2e10$ molecules/ml
- Area of 20 μm x 60 μm , each protein 10nm x 10nm \rightarrow $\sim 1e8$ proteins

Polymer/Silicon Cantilever Sensors

- Environmentally sensitive micro-patterned polymer structures on cantilevers
- Hydrogel patterned on cantilever and then exposed to varying pH



- $\Delta\text{pH} = 1-10\text{e-}5$
- $\text{pH} = 6.5 \rightarrow \sim 1.9\text{e}5 \text{ H}^+$ in $1000\mu\text{m}^3$
- $\Delta\text{pH} = 5\text{e-}4 \rightarrow$ change of $\sim 150 \text{ H}^+$

2. Microcantilever Mass Sensors

Unloaded Resonant Frequency :

$$f_0 = \frac{1}{2\pi} \sqrt{\frac{k}{m^*}}$$

Spring constant for a rectangular shaped cantilever beam: $k = \frac{Et^3w}{4l^3}$

Loaded Resonant frequency : $f_1 = \frac{1}{2\pi} \sqrt{\frac{k}{m^* + \delta m}}$

δm is the added mass

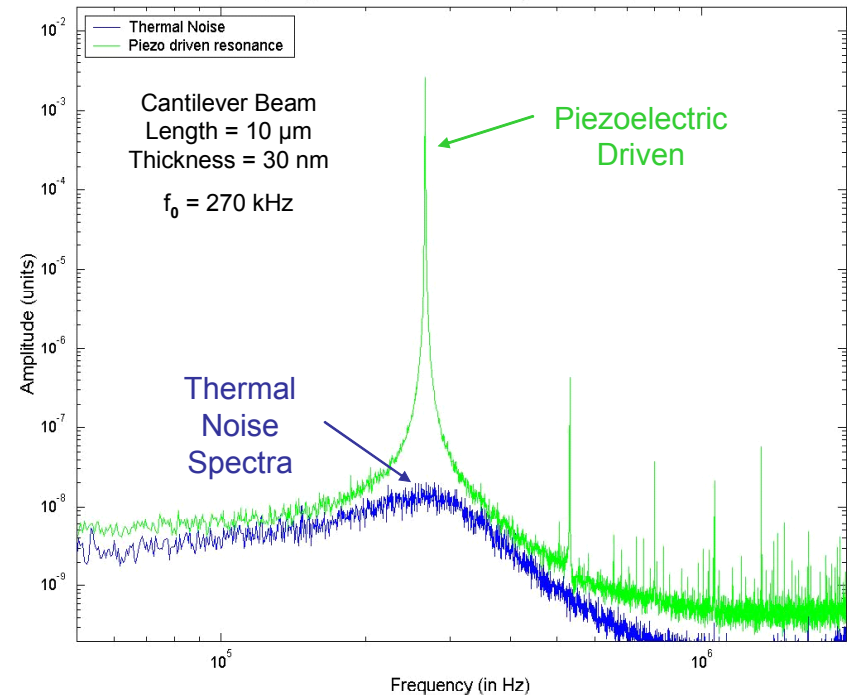
$$\Delta m = \frac{k}{4\pi^2} \left(\frac{1}{f_1^2} - \frac{1}{f_0^2} \right)$$

- k = spring constant
- m = mass of cantilever
- f_0 = *unloaded resonant frequency*
- f_1 = *loaded resonant frequency*

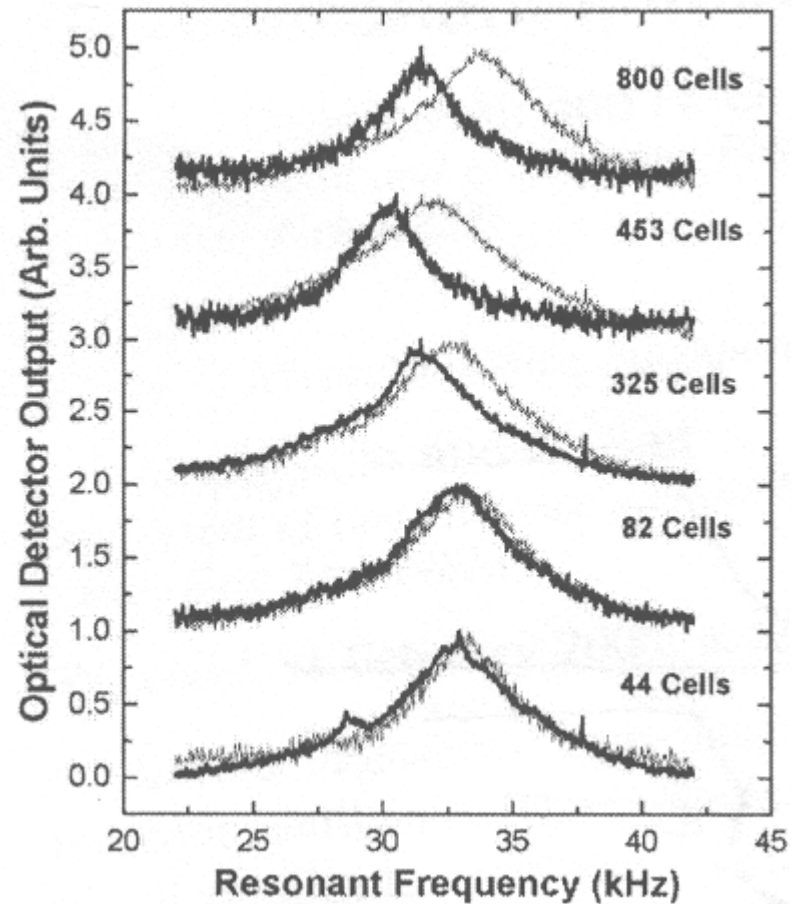
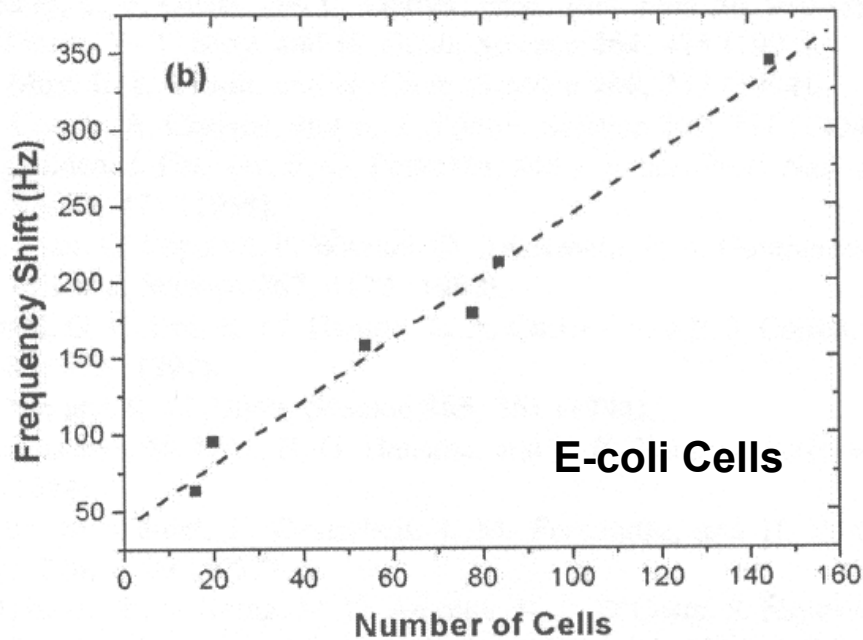
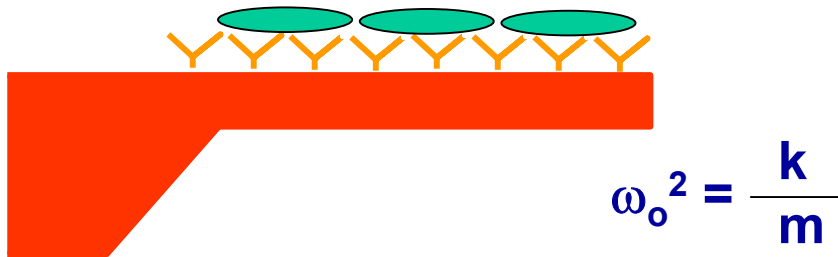
Mass Change Detection



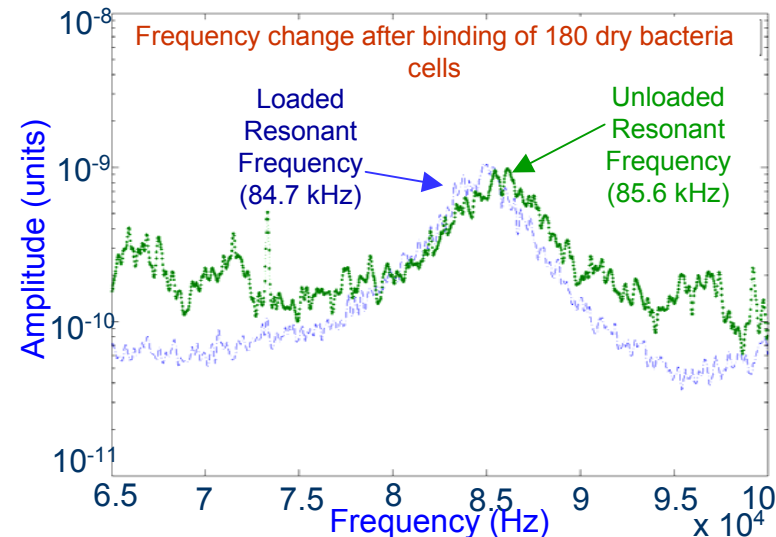
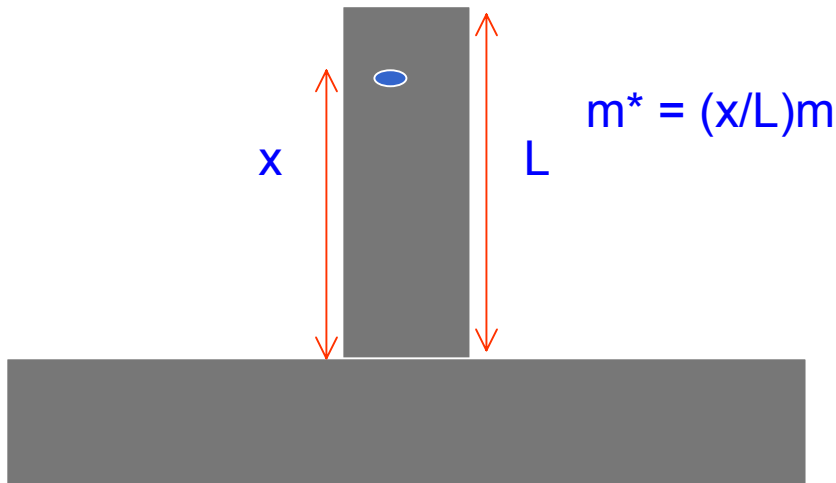
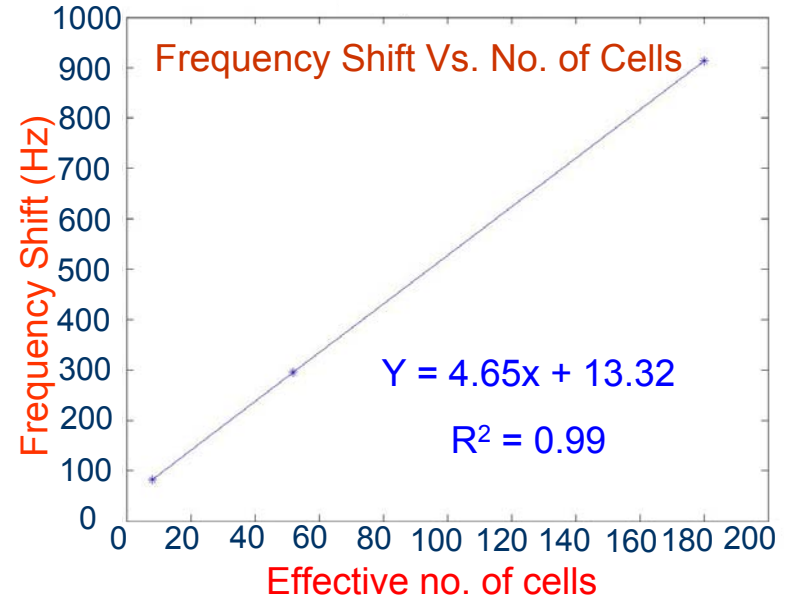
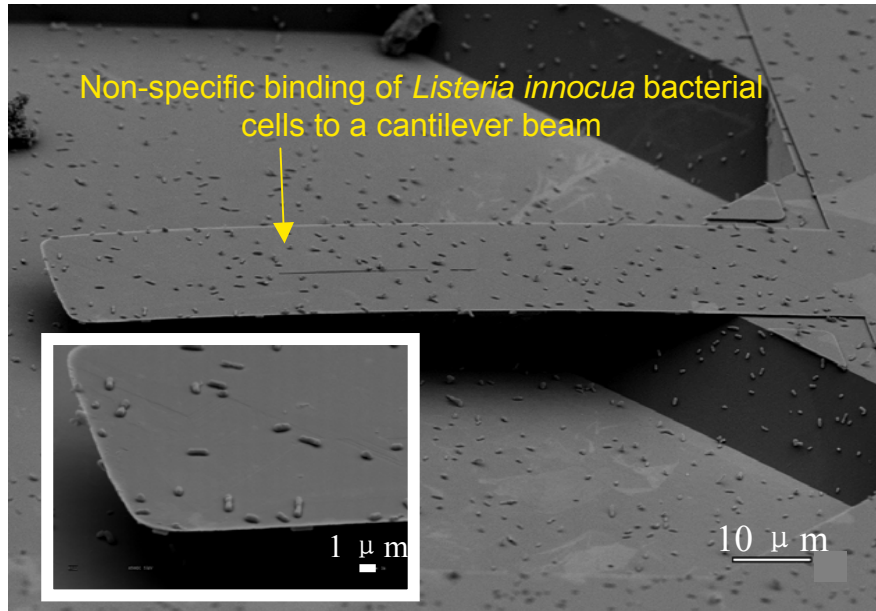
PSD comparing measurements done using thermal and piezo driven



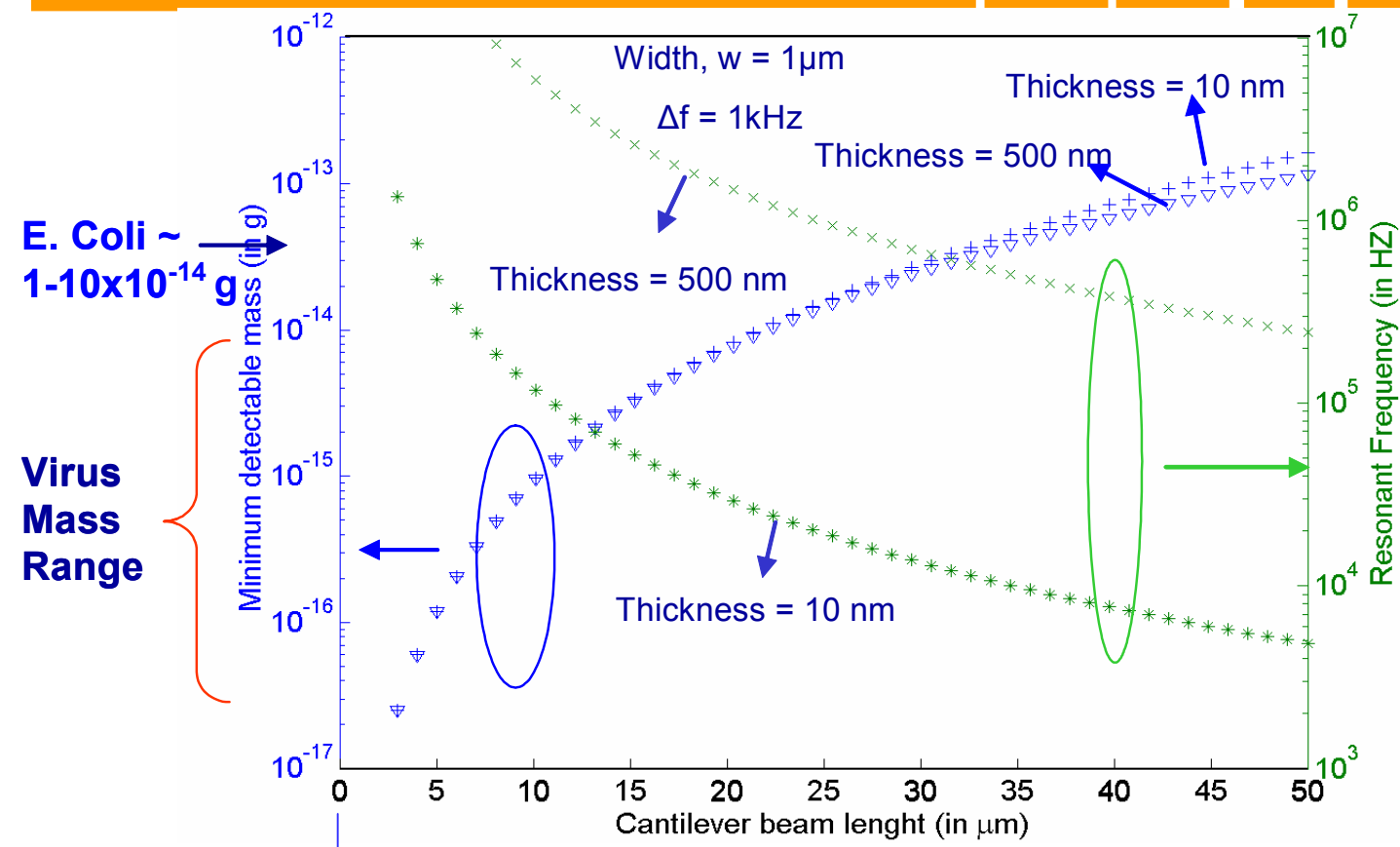
Detection of Bacterial Mass



Detection of Listeria Cell Mass



Minimum Detectable Mass



E. Coli ~
1-10x10⁻¹⁴ g

Virus Mass Range

100kDa Protein

DNA bp ~ 10⁻²¹ g

$$\delta m = 0.24 \cdot l \cdot w \cdot t \cdot \rho \cdot \left(\frac{1}{\left(1 - \frac{2\pi\delta f (0.98)l^2}{t} \sqrt{\frac{\rho}{E}} \right)^2} - 1 \right)$$

Minimum Detectable Mass

- The frequency measurement is limited by thermo-mechanical noise on the cantilever beam.

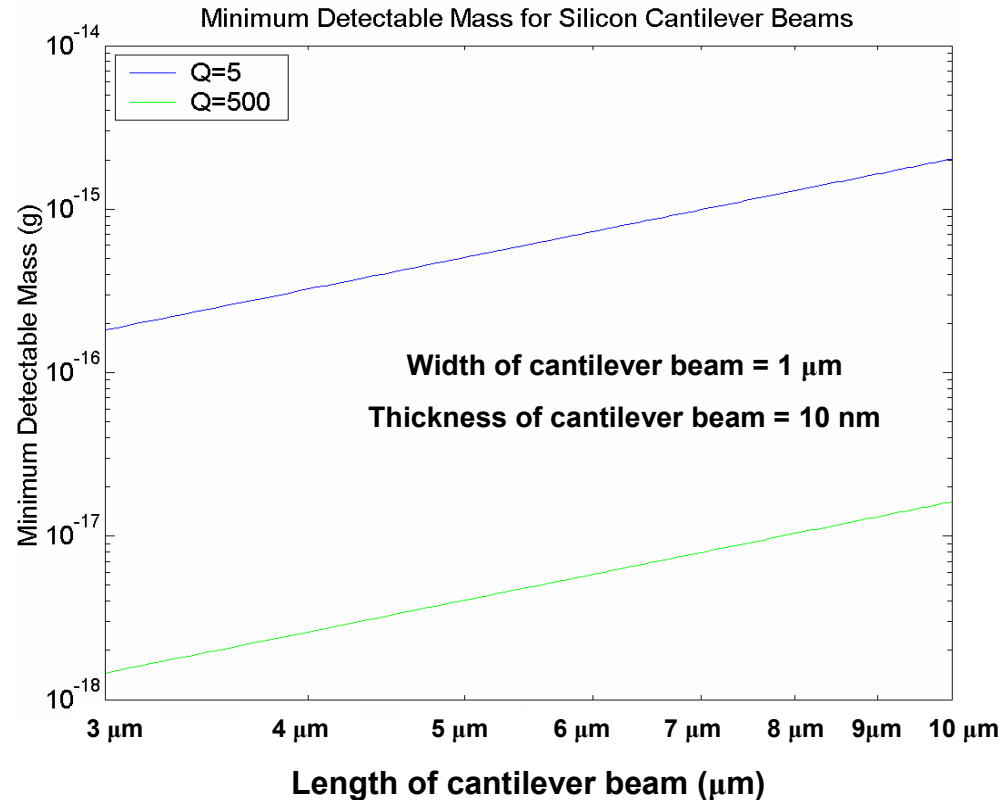
- Minimum Detectable Frequency,

$$\Delta f_{\min} = \frac{1}{A} \sqrt{\frac{f_0 k_B T B}{2 \pi k Q}}$$

- Minimum Detectable Mass,




$$\Delta m_{\min} = \frac{1}{A} \sqrt{\frac{4 k_B T B}{Q}} \frac{m_{\text{eff}}^{5/4}}{k^{3/4}}$$

- k_B = Boltzmann constant
- T = Temperature in Kelvin
- B = Bandwidth measurement, (~ 1 kHz)
- Q can increase by 100X by driving the cantilevers



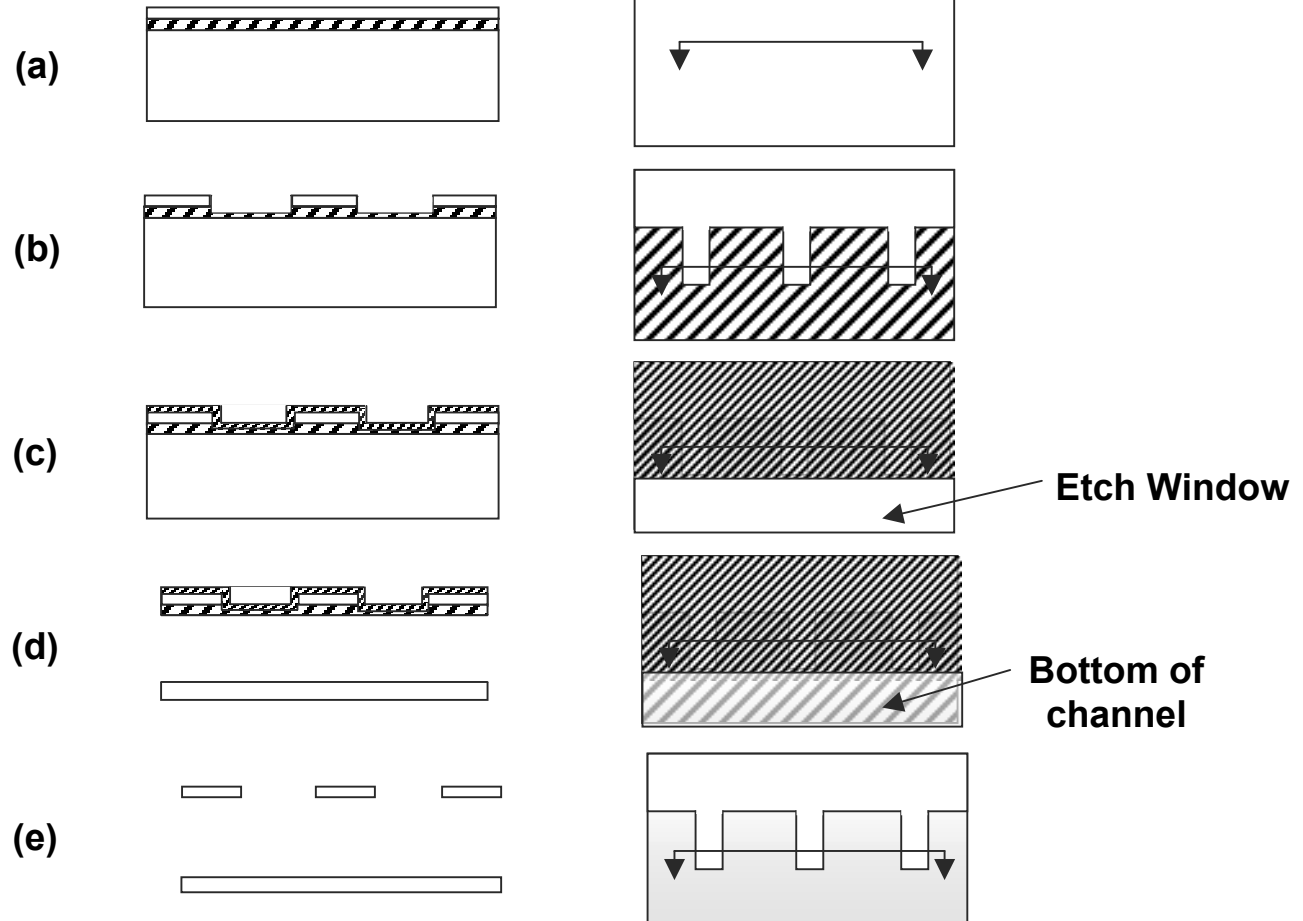
Fabrication Process Flow

Materials Legend

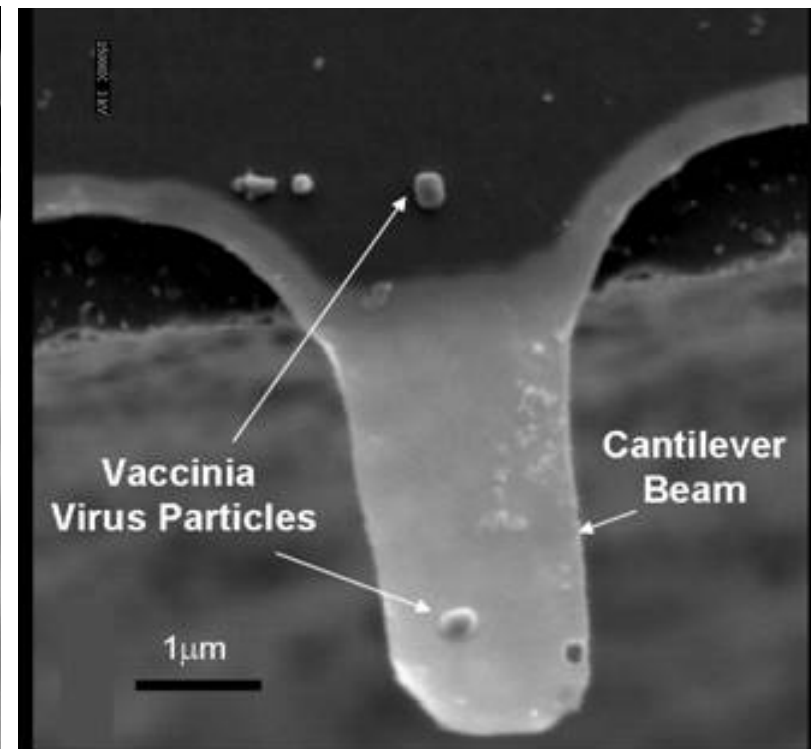
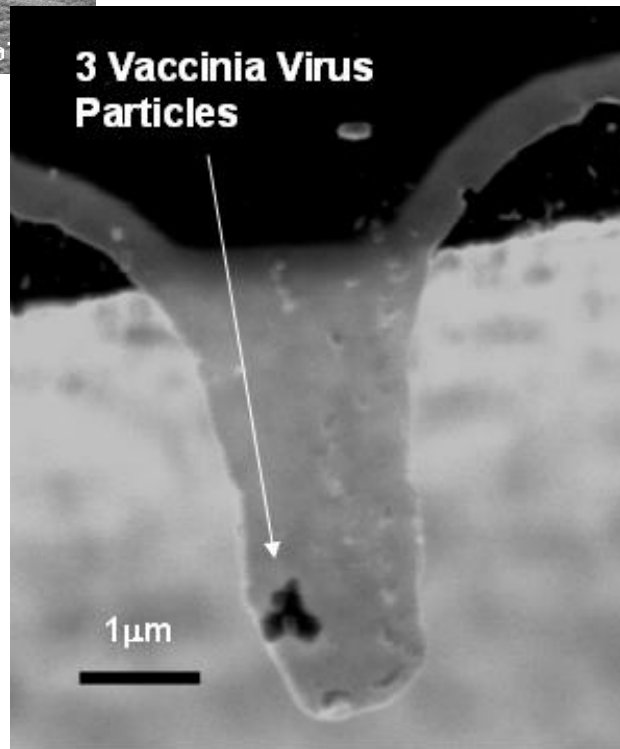
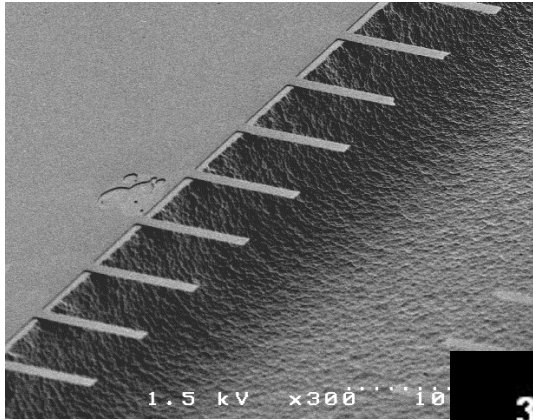
-  Silicon
-  Silicon dioxide
-  PECVD Silicon dioxide

Cross-sectional view

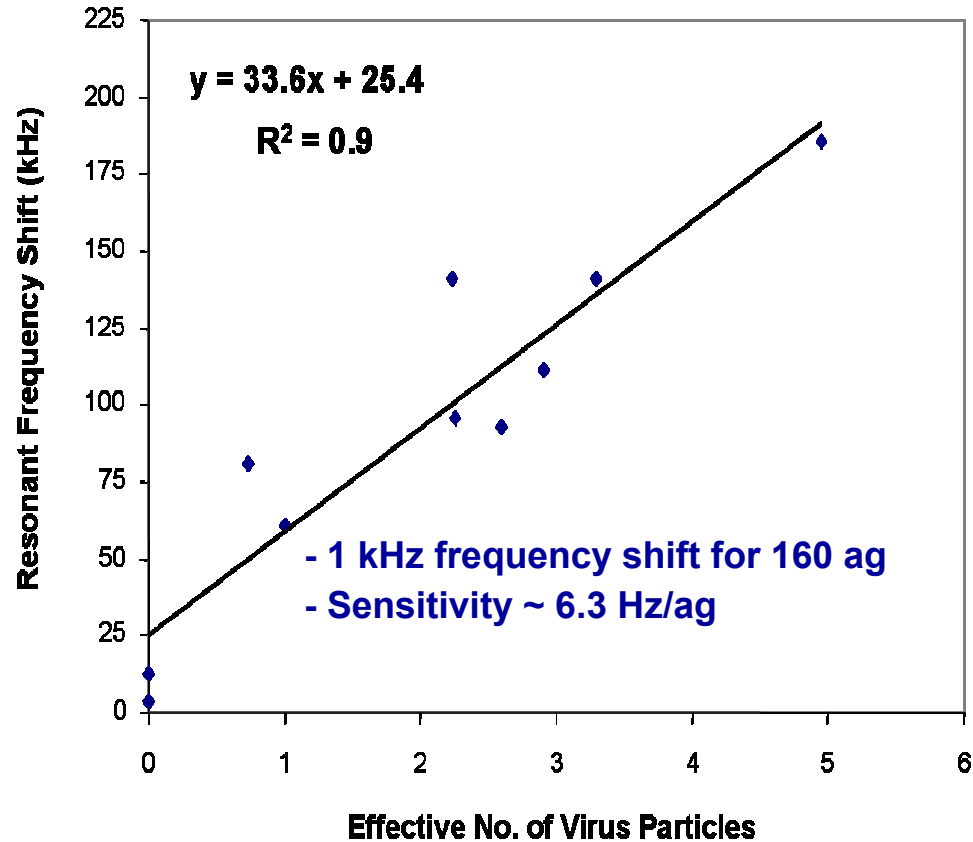
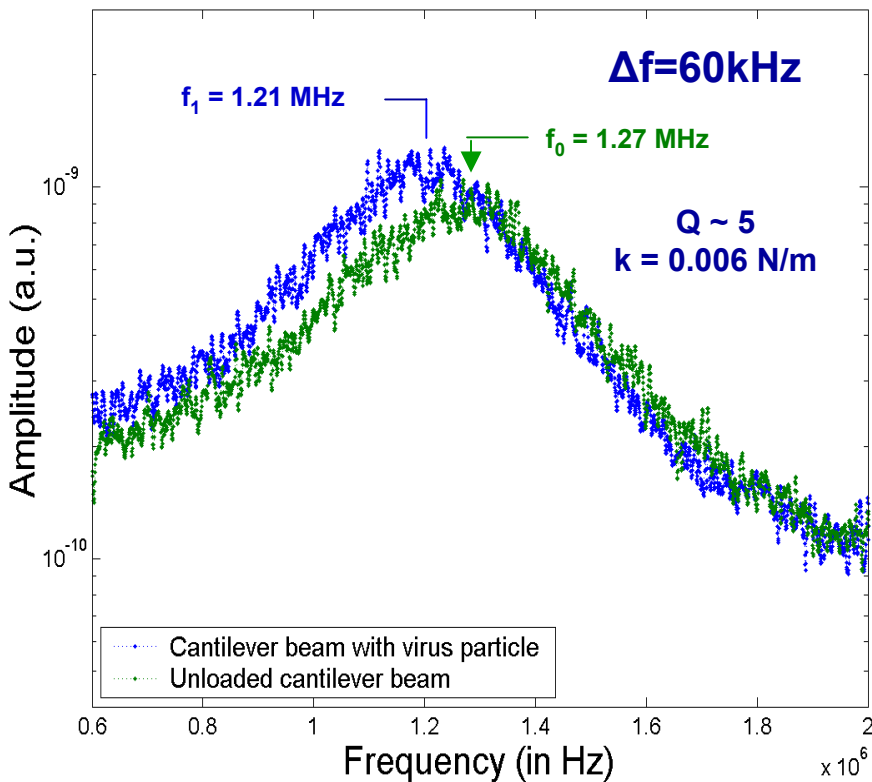
Top view



SEM Pictures of Cantilevers

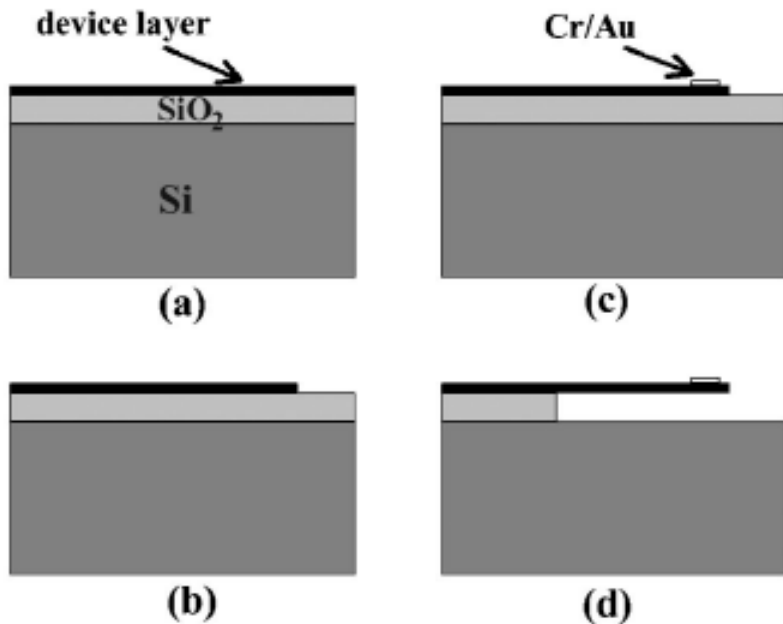


Frequency Shift vs. No. of Particles



- Average mass of Vaccinia Virus ~ 9.5 fg
- Work on going to integrated concentration elements
- Integrated Abs on cantilevers

Mass of Molecules



To probe the amount of thiolate binding to the Au contacts, we have measured the frequency spectra before and after the thiolate self-assembly. Figure 14 shows the measured shift in the resonant frequency for DNP-PEG4-C11thiol binding on 50- and 400-nm-diam Au contacts. The measured frequency shifts were 125 Hz and 1.10 kHz, corresponding to calculated masses of 6.3 and 213.1 ag, respectively.

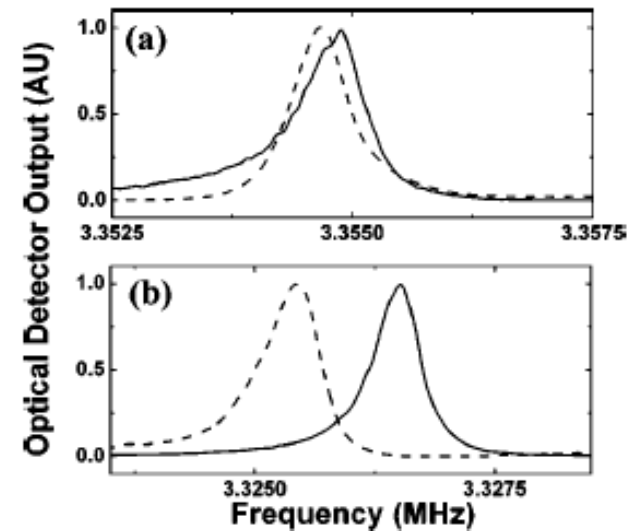
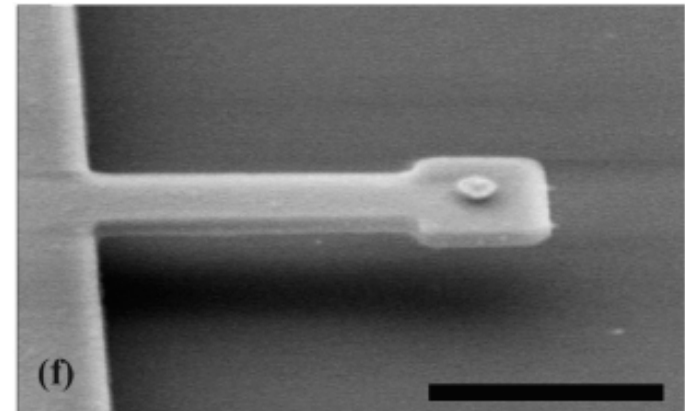
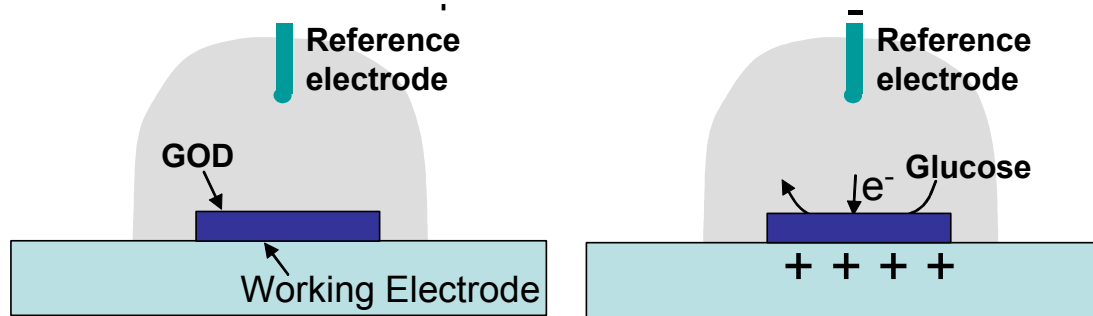


FIG. 14. Experimentally measured frequency spectra before (solid line) and after (dashed line) the adsorption of the thiolate on (a) 50- and (b) 400-nm-diam Au contact. Rectangular beam dimensions were $l=10\ \mu\text{m}$, $w=1\ \mu\text{m}$, and $t=250\ \text{nm}$.

Electrical/Electrochemical Detection

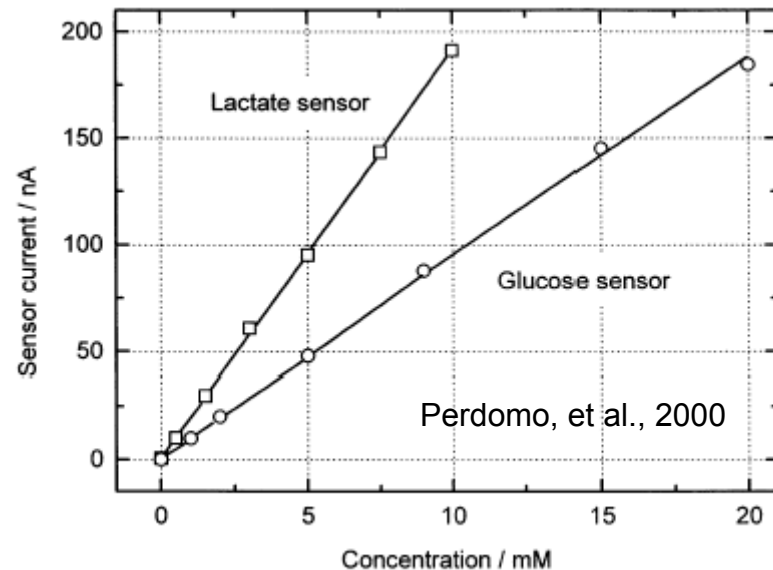
1. amperometric biochips, which involves the electric current associated with the electrons involved in redox processes,
2. potentiometric biochips, which measure a change in potential at electrodes due to ions or chemical reactions at an electrode (such as an ion Sensitive FET), and
3. conductometric biochips, which measure conductance changes associated with changes in the overall ionic medium between the two electrodes.

1. Amperometric Detection



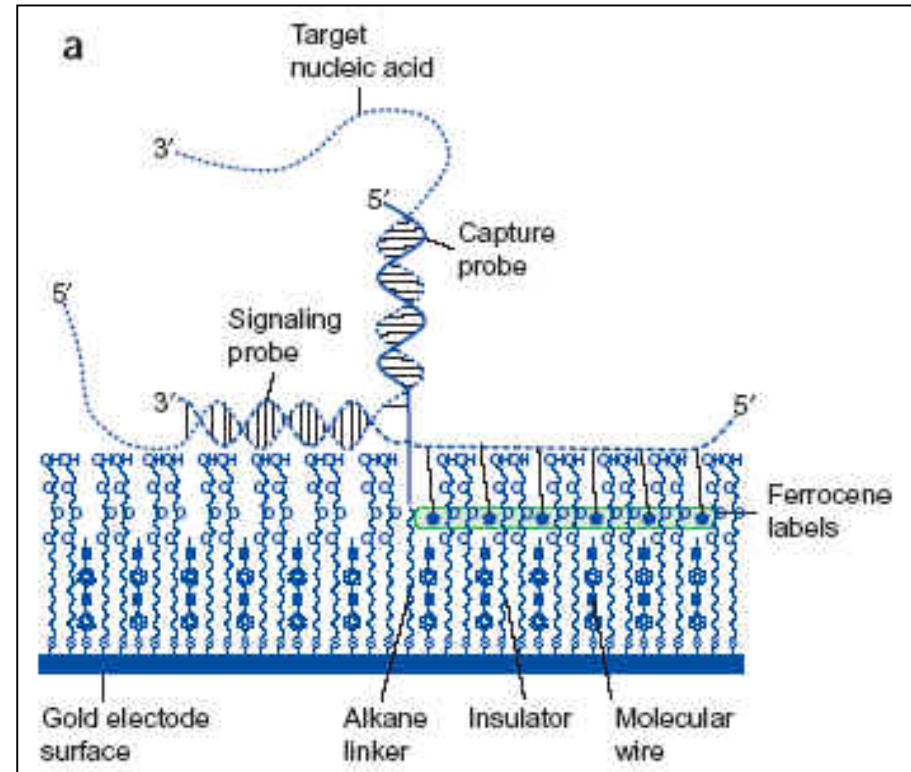
hydrogen peroxide is reduced at -600mV at Ag/AgCl anode reference electrode.

- Detection of Glucose, Lactate, Urea, etc.
- Enzyme entrapped in a gel
- Surface regeneration and sensor reusability



Detection of DNA Hybridization

- Capture probes are attached to electrodes.
- Target DNA binds to complementary probes
- DNA sequences, called signaling probes, with electronic labels attach to them (ferrocene-modified DNA oligonucleotides, $E_{1/2}$ of 0.120 V vs. Ag/AgCl, act as signaling probes).
- Binding of the target sequence to both the capture probe and the signaling probe connects the electronic labels to the surface.
- The labels transfer electrons to the electrode surface, producing a characteristic signal.

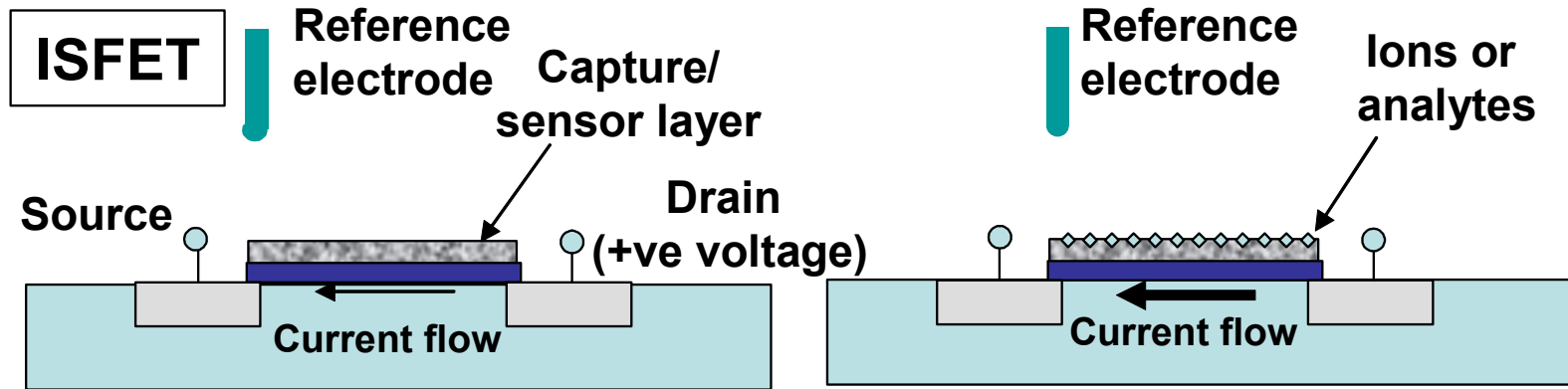


Umek, et al. J. Molecular Diagnostics, 3, 74-84, 2001

Drummond, Hill, Barton, Nature Biotech, v21, n10, Oct 2003, p1192

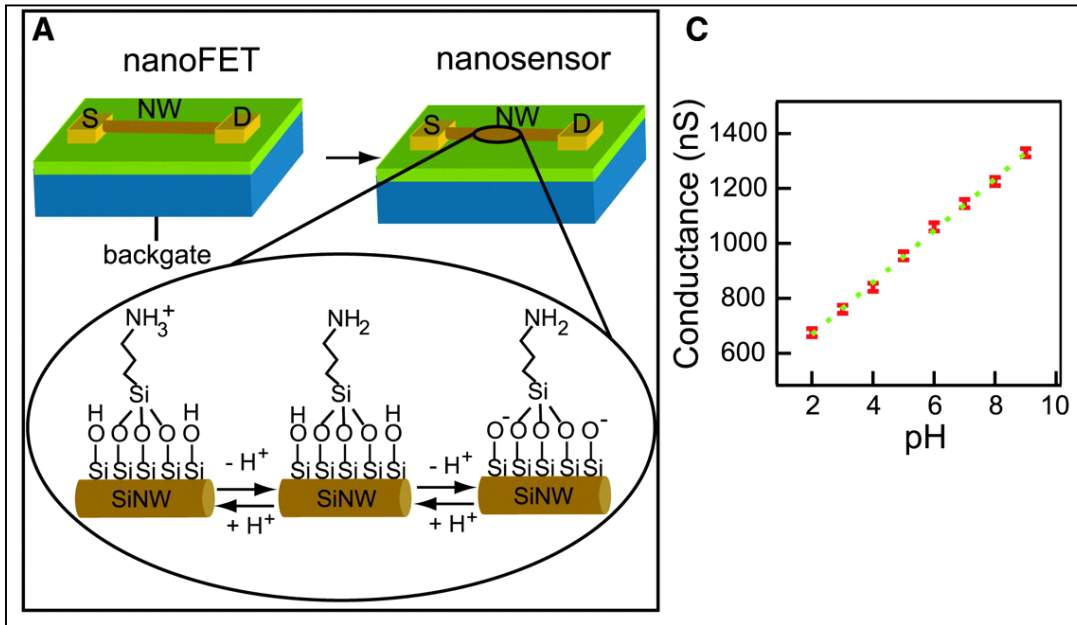
http://www.motorola.com/lifesciences/esensor/tech_bioelectronics.html

2. Potentiometric Sensors

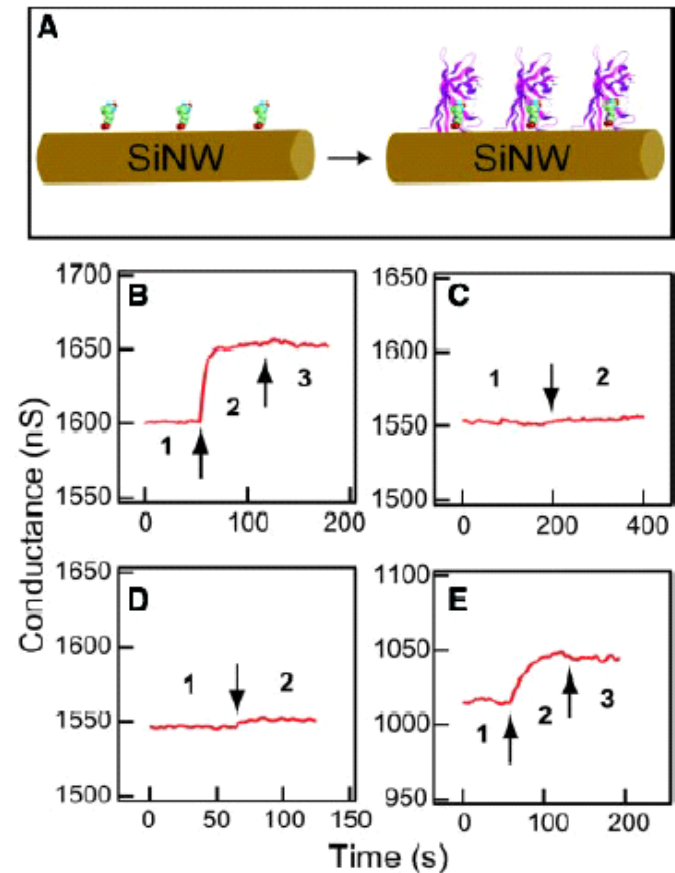


- ISFETs, ChemFETs, etc.
- Potential difference between the gate and the reference electrode in the solution
- Change in potential converted to a change in current by a FET or to a change in capacitance in low doped silicon
- Gate material is sensitive to specific targets
- pH, Ions, Charges

Nanoscale pH Sensors



- Label Free !!
- Detection of pH change
- Detection of protein binding

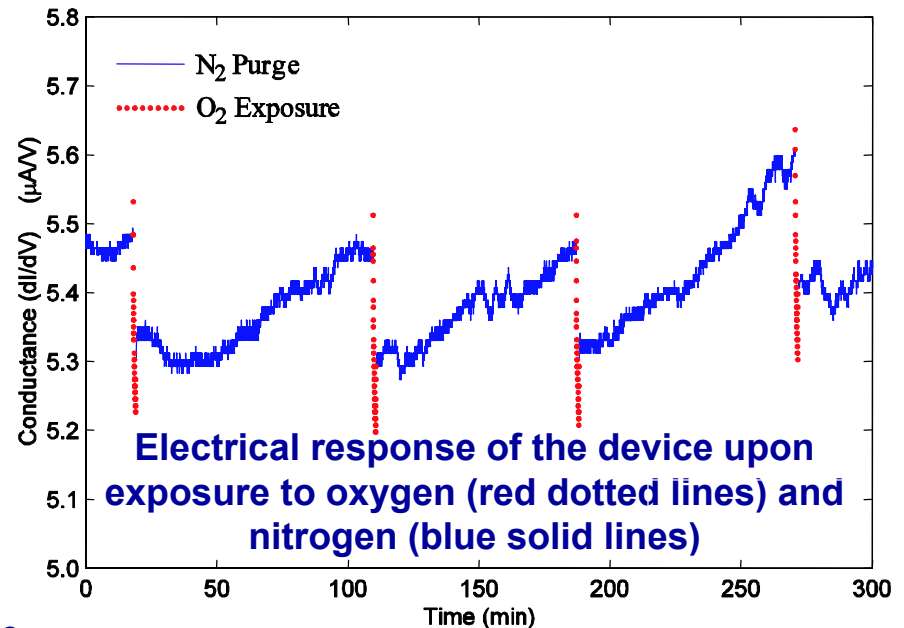
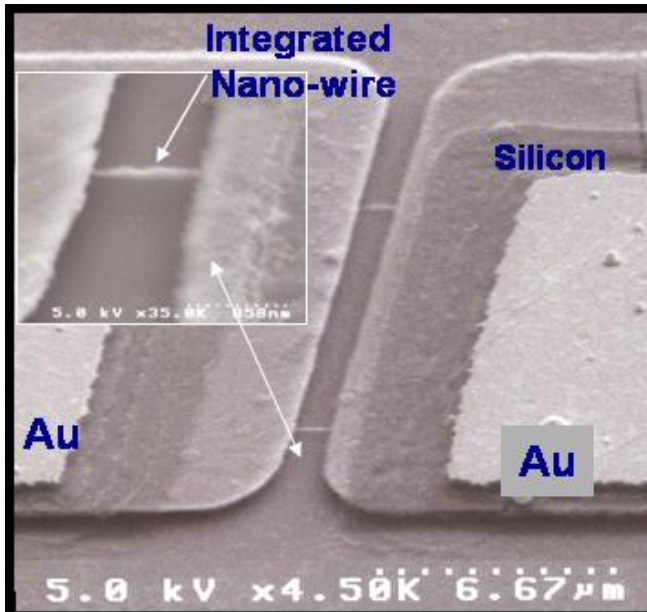
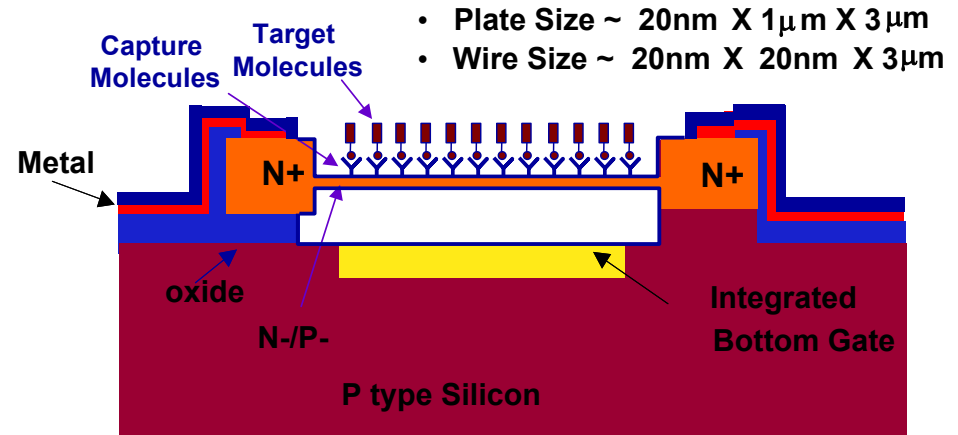


- Streptavidin binding detection down to at least **10 pM**.
- Substantially lower than the nanomolar range demonstrated by other procedures.

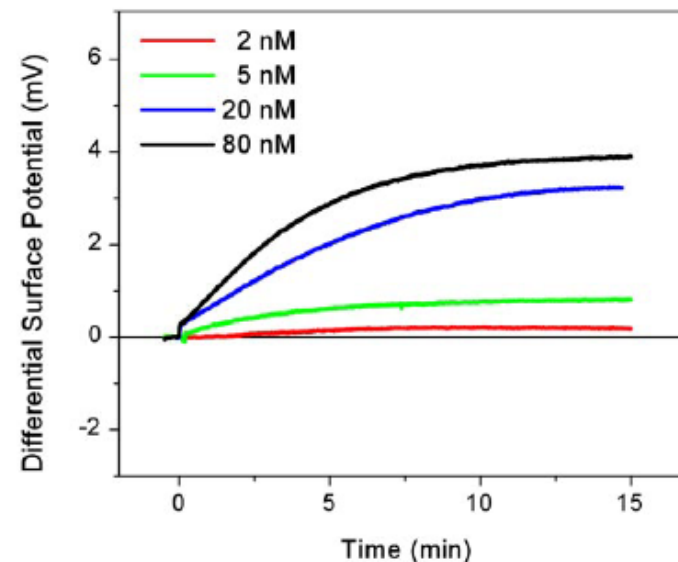
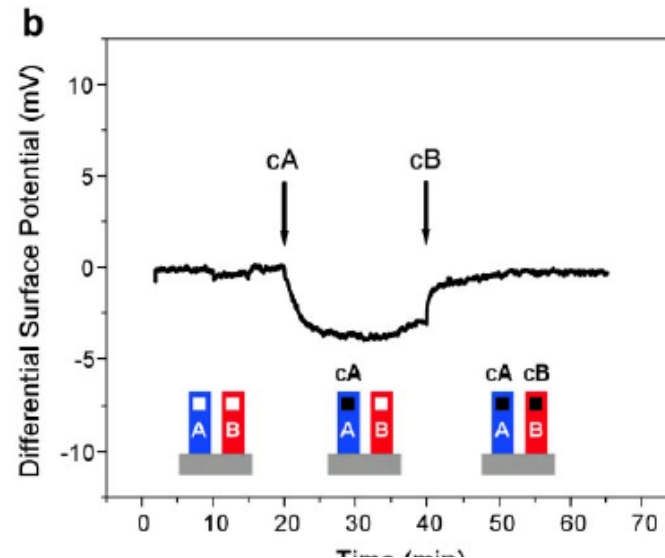
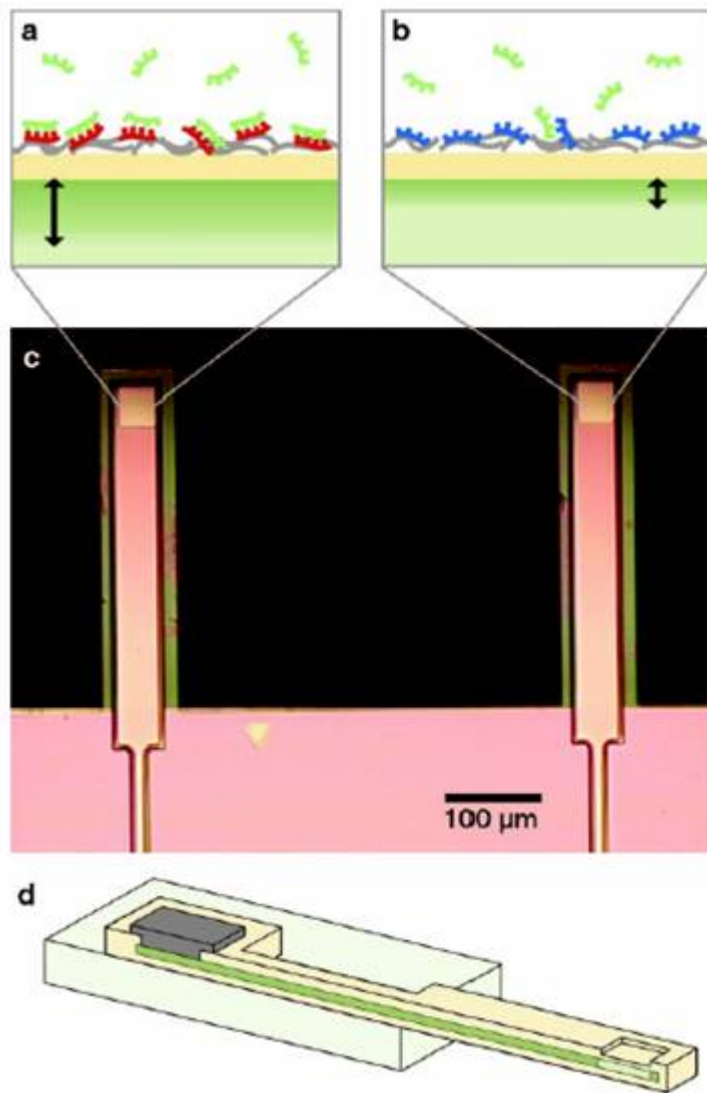
Integrated Silicon Nanowire Sensors

Objectives:

- Bio-sensors with electronic output
- Capability of dense arrays integrated with ULSI silicon
- Direct Label Free Detection of DNA and Proteins

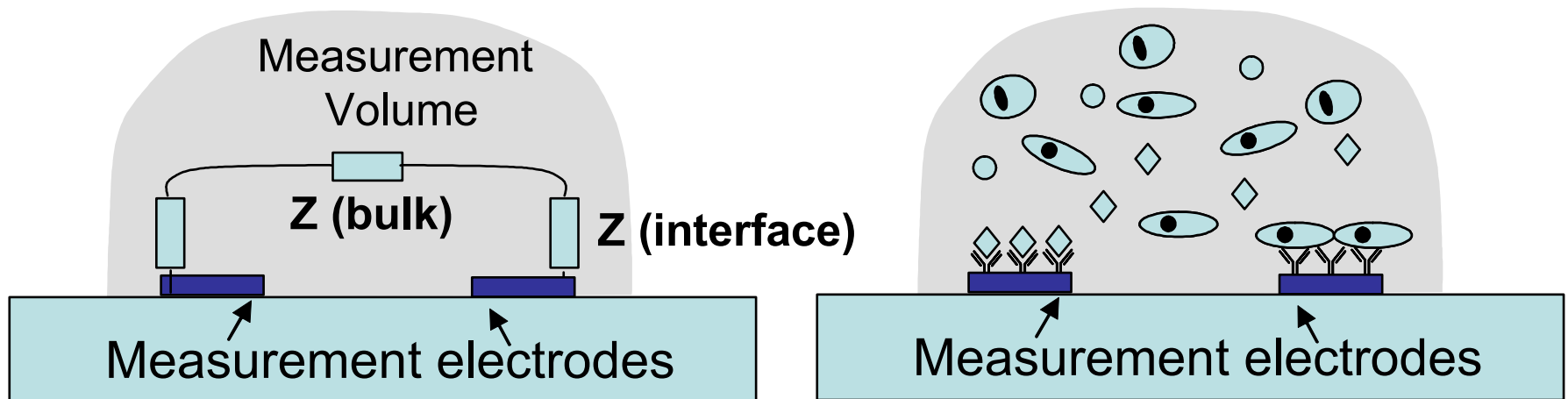


Field Effect Sensing of DNA



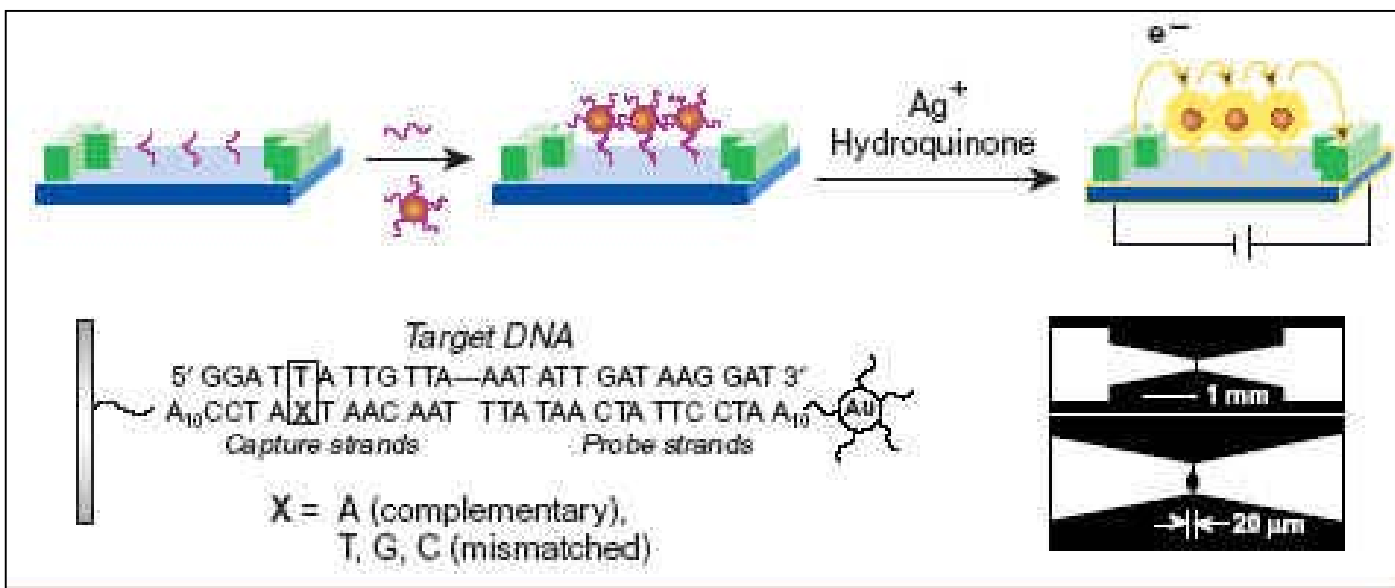
3. Conductometric Biochips

- Conductometric sensors measure the changes in the electrical impedance between two electrodes, where the changes can be at an interface or in the bulk region and can be used to indicate biomolecular reaction between DNA, Proteins, and antigen/antibody reaction, or excretion of cellular metabolic products.



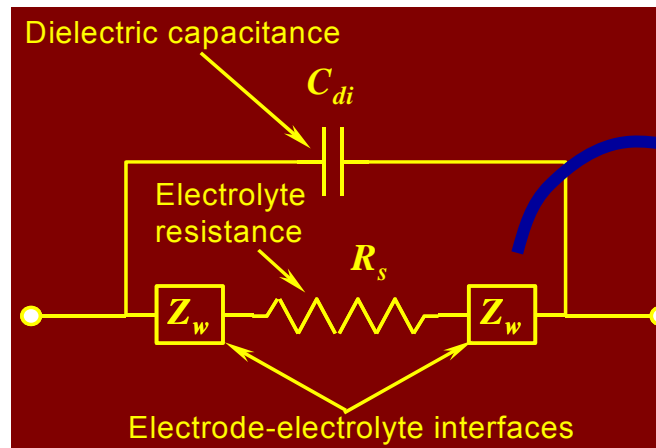
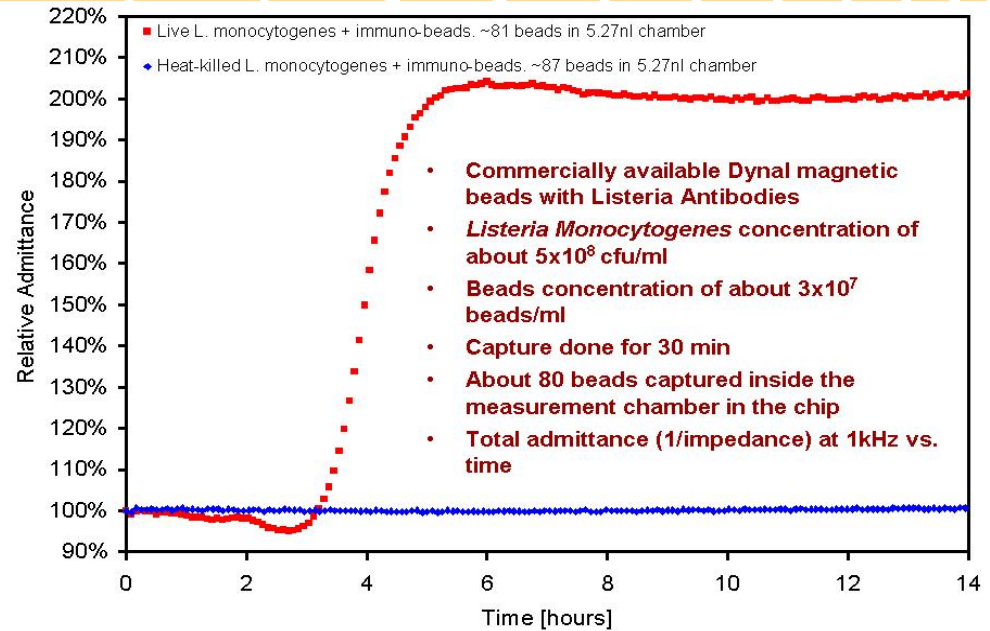
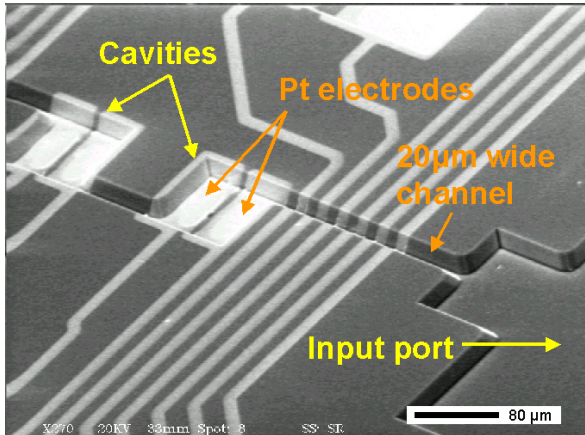
Nanoparticle Mediated DNA Detection

- Au nanoparticles assemble between two electrodes if DNA is hybridized
- Silver staining of the Au nanoparticles
- Conductance changes between micro-scale electrodes indicate DNA hybridization
- Sensitivity of 5×10^{-13} M shown



Micro-fluidic Devices for Conductance Detection of Bacterial Metabolism

Detection of Cell Growth by measuring their metabolic activity in micro-fluidic devices



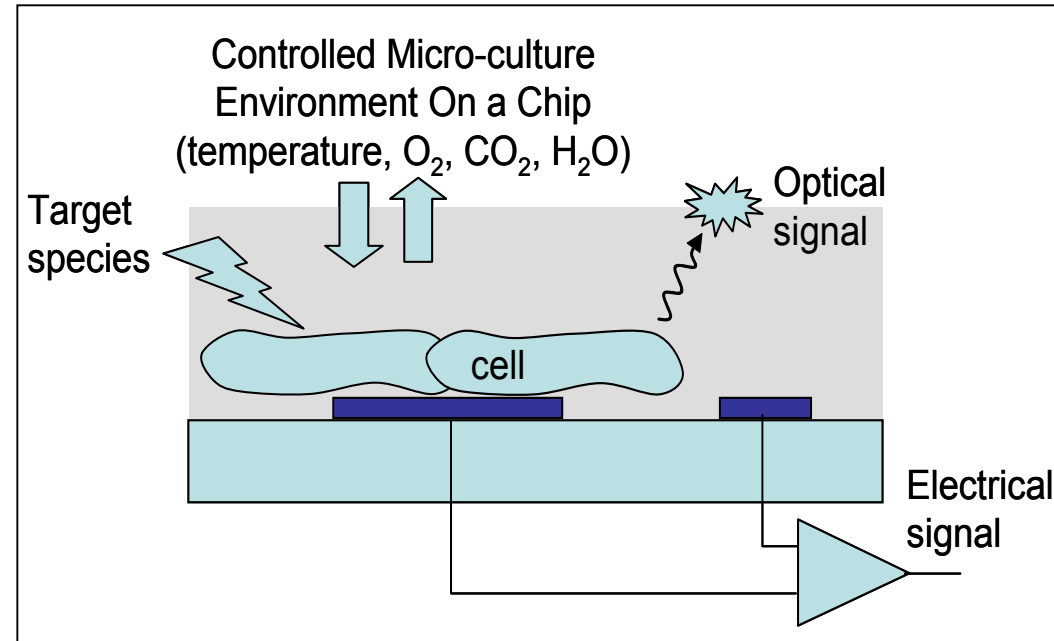
Electrode-Electrolyte Interface Model:

$$Z_w = \frac{1}{(j\omega)^n B}$$

Constant-angle impedance

4. Cell-Based Sensors/Biochips

- The transductions of the cell sensor signals maybe achieved by:
 - the measurement of transmembrane and cellular potentials,
 - impedance changes,
 - metabolic activity,
 - analyte inducible emission of genetically engineered reporter signals, and
 - optically by means of fluorescence or luminescence.

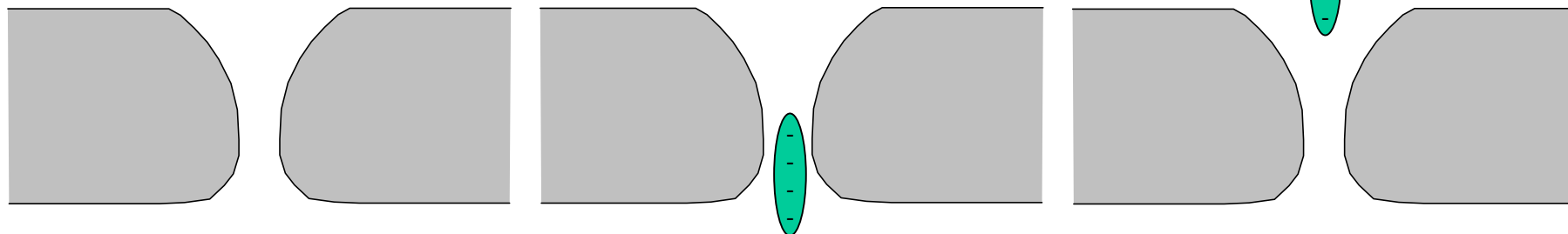


L. Bousse, Whole cell biosensors, *Sensors and Actuators B (Chemical)*, Vol. B34, No. 1-3, August 1996, pp. 270-5.
J.J. Pancrazio, J.P. Whelan, D.A. Borkholder, W. Ma, D.A. Stenger, Development and application of cell-based biosensors, *Annals of Biomedical Engineering*, Vol. 27, No. 6, November 1999, pp. 697-711.
D.A. Stenger, G.W. Gross, E.W. Keefer, K.M. Shaffer, J.D. Andreadis, W. Ma, J.J. Pancrazio, Detection of physiologically active compounds using cell-based biosensors, *Trends in Biotechnology*, Vol. 19, No. 8, August 1, 2001, pp. 304-309.

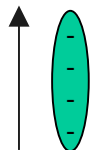
5. Micro/Nano-scale Coulter Counter

+

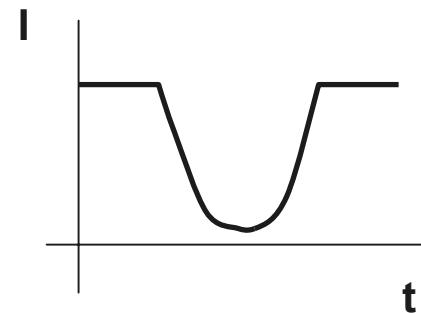
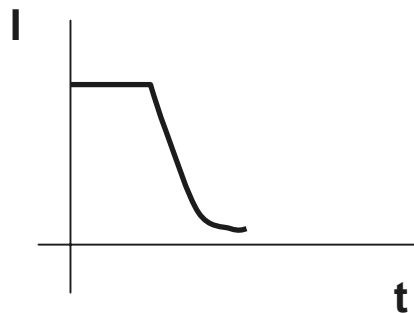
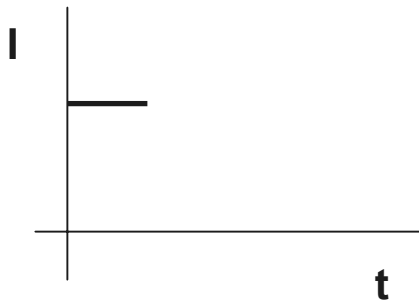
Trans
chamber



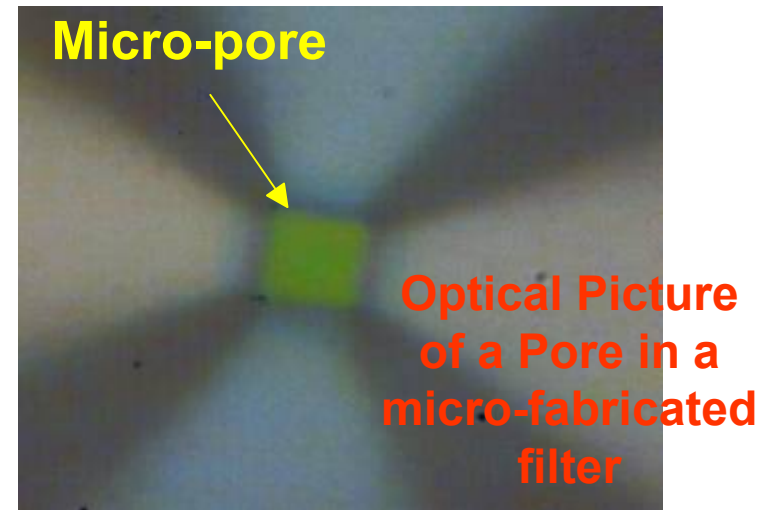
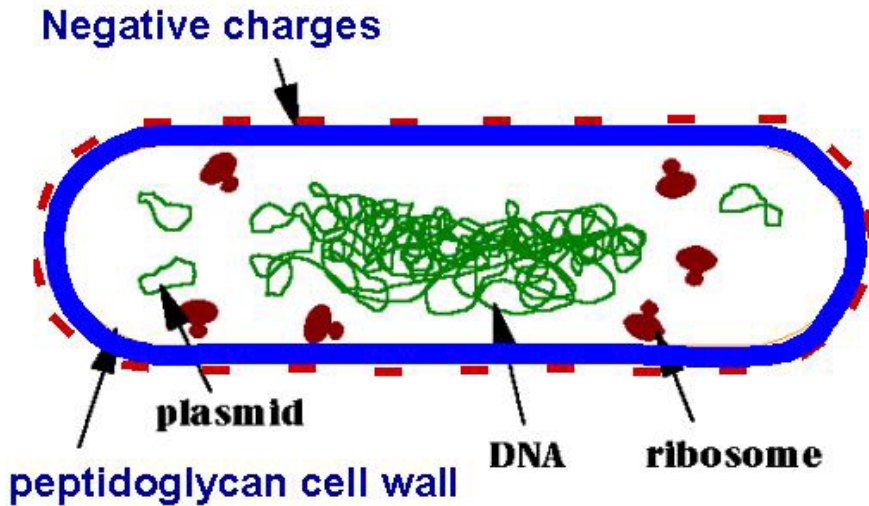
-



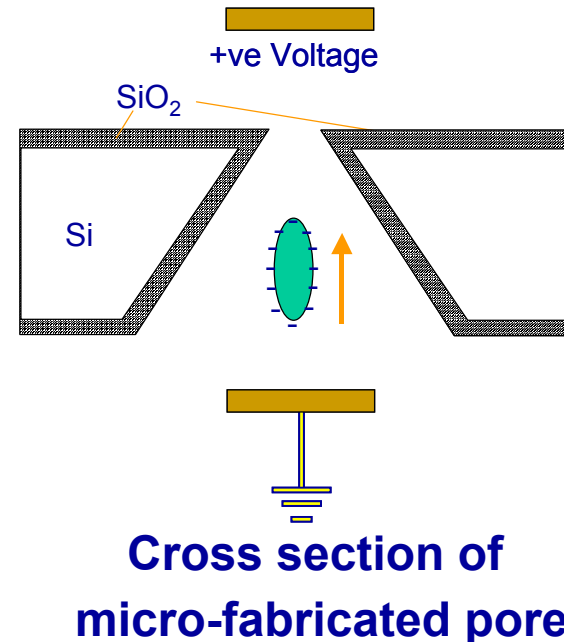
Cis
chamber



Micro-pore for cellular studies

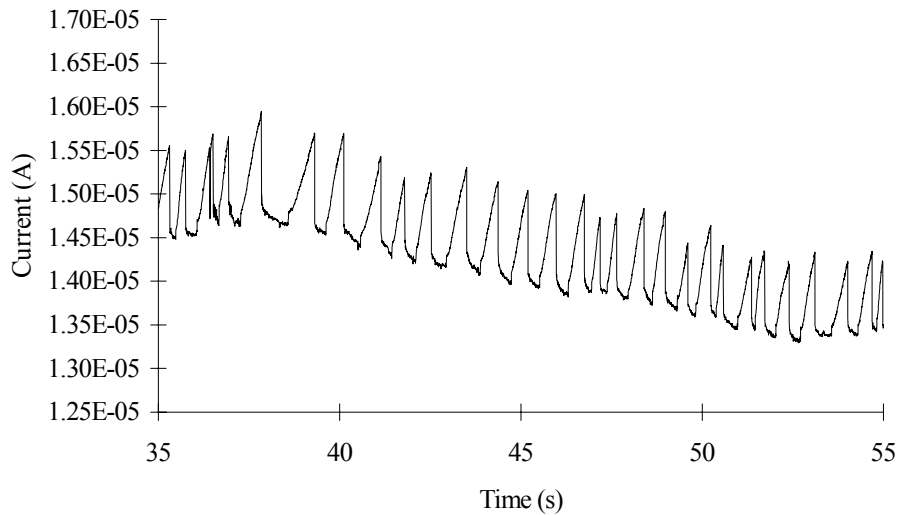


- Micro-devices for single cell characterization – utilize the charge properties
- Micro-fabricate a pore where single entity can pass

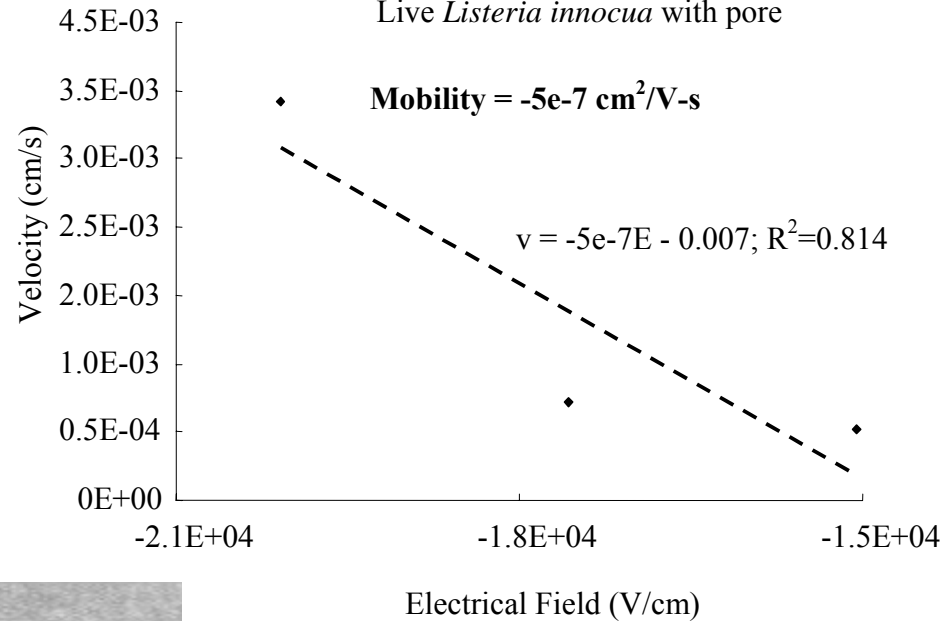


Microscale Coulter Counter

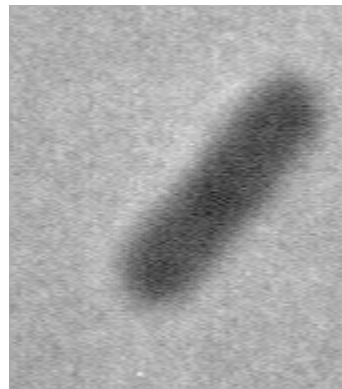
I-T Diagram for Live *Listeria*, 1e8/ml, V = 40 V, 05112010



Velocity (cm/s) vs. Electrical Field (V/cm)
Live *Listeria innocua* with pore

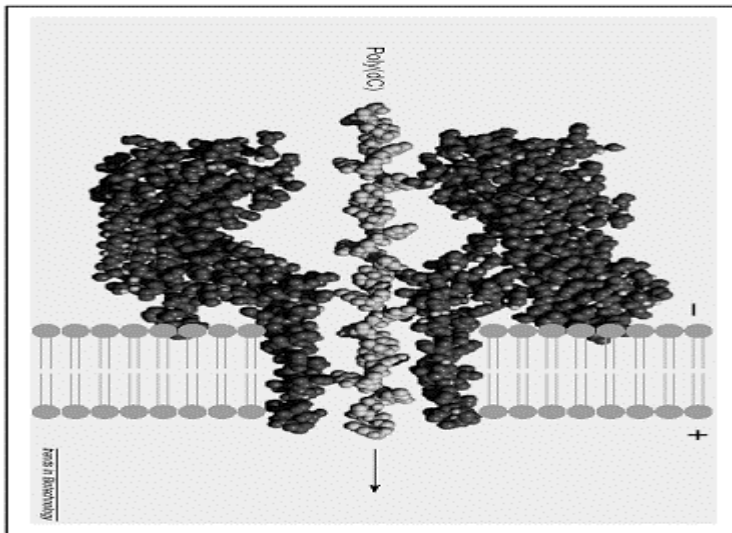


Live *Listeria innocua*
with a well-defined
cell wall



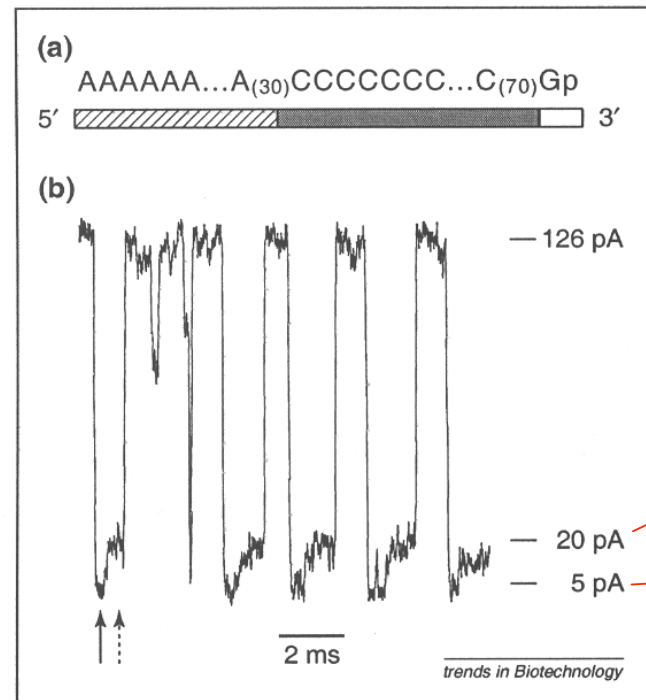
Nanoscale DNA Coulter Counter

- α -hemolysin channel, a biological protein based-pore, was utilized.
- Pore size is 2.6 nm.
- Both RNA and DNA molecules were observed traversing the nanochannel.



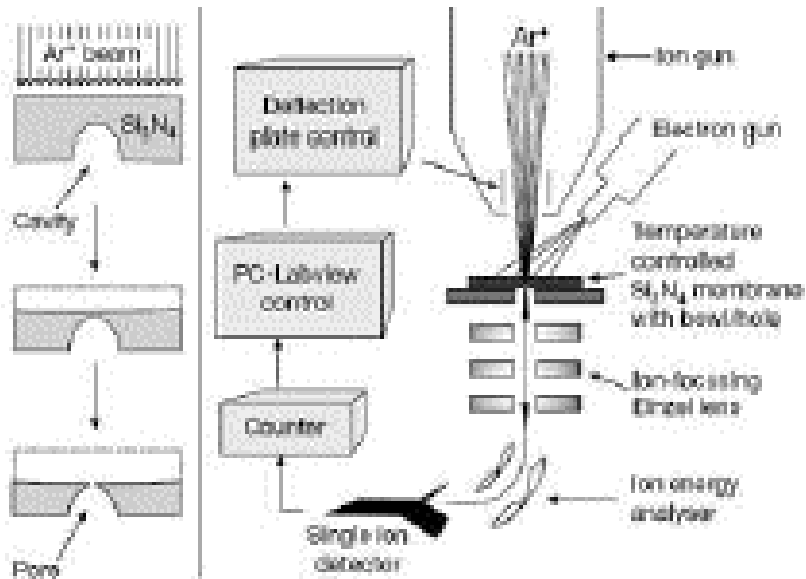
α -hemolysin nanochannel

The model of DNA passing through an α -hemolysin channel.

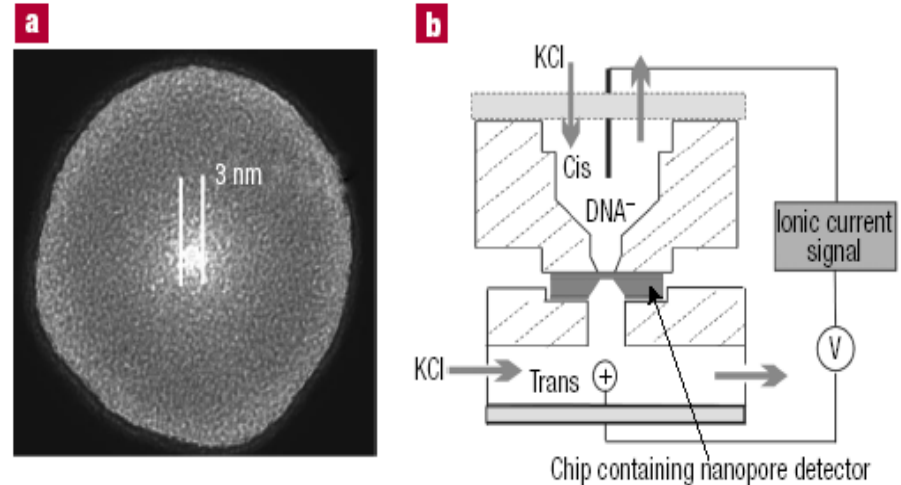


Fabrication Techniques

- Solid-state based nanopore. Made in silicon nitride membrane.
- Pore size: 3 nm and 10 nm.
- The relation among DNA lengths and translocation times and applied biases were determined.

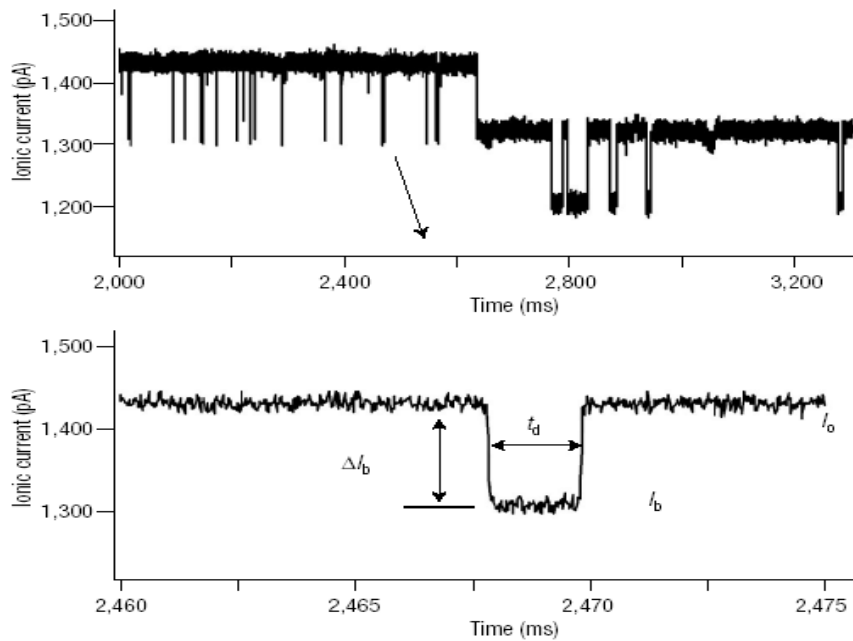


The fabrication of Li's nanopore. From *Li et. al. Nature, 2001.*

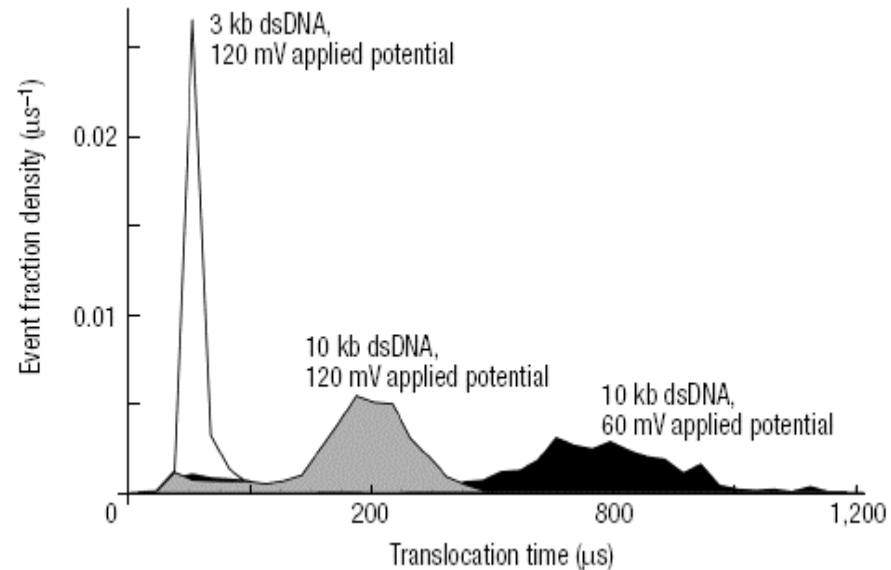


TEM of Li's nanopore. b. DNA measurement setup in Li's work. From *Li et. al. Nature Materials, 2003*

DNA Translocation



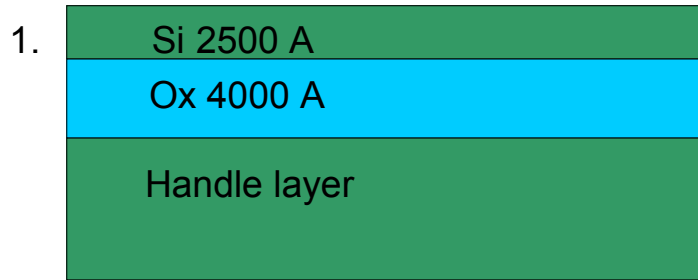
Current fluctuations when DNA was passing through the pore



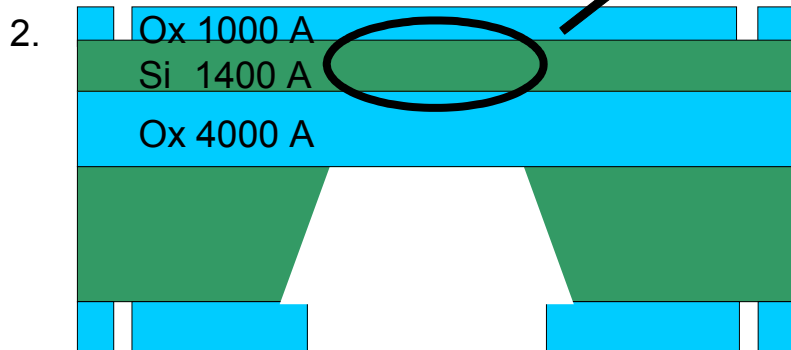
Histograms of relation among DNA lengths, translocation times and applied biases.

Silicon Based Nanopore

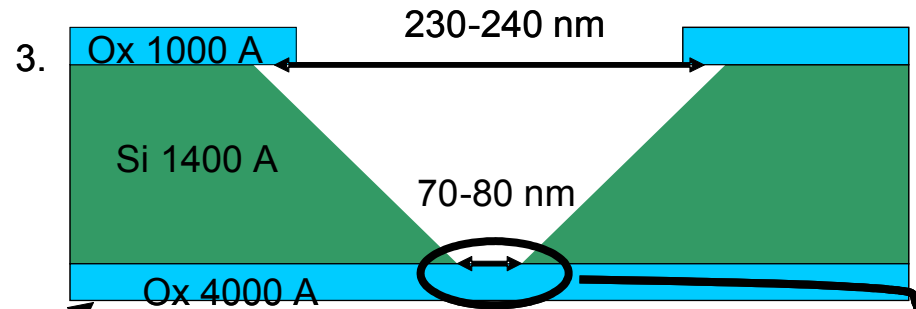
(Not to scale)



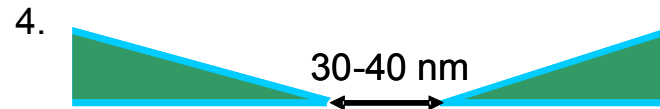
Start with a (100) 4 inch SOI wafer.
Thickness : 525 μ m. SOI : 250 nm,
Buried oxide layer: 400 nm.



Grow thermal oxide on wafer surface and open etch window to etch through the handle layer. Etch stops on buried oxide layer.



On SOI layer, open another etch window to etch through the SOI layer. Etch stops on buried oxide layer.

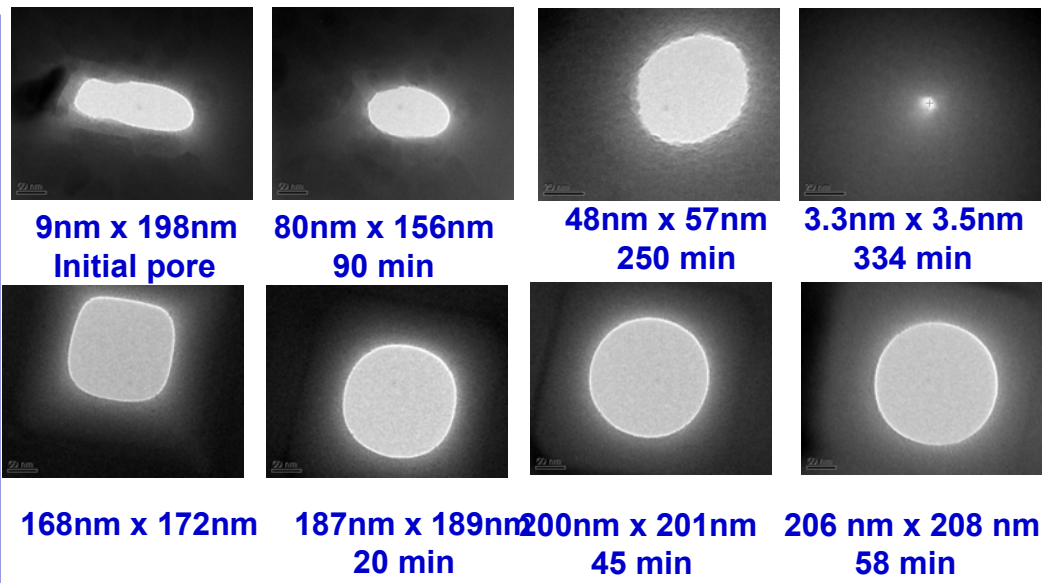
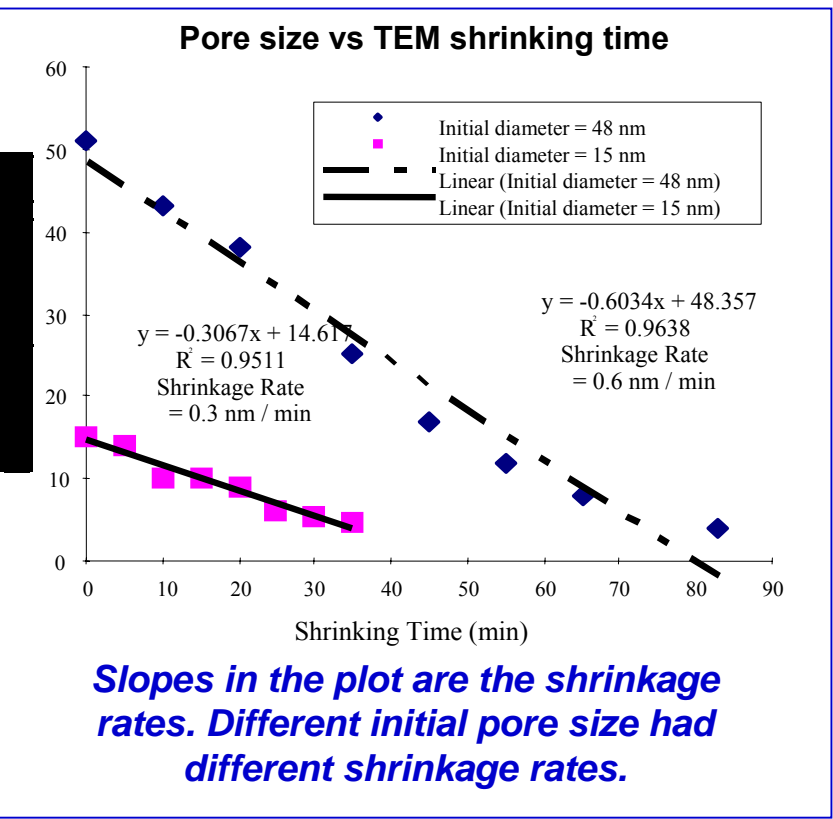
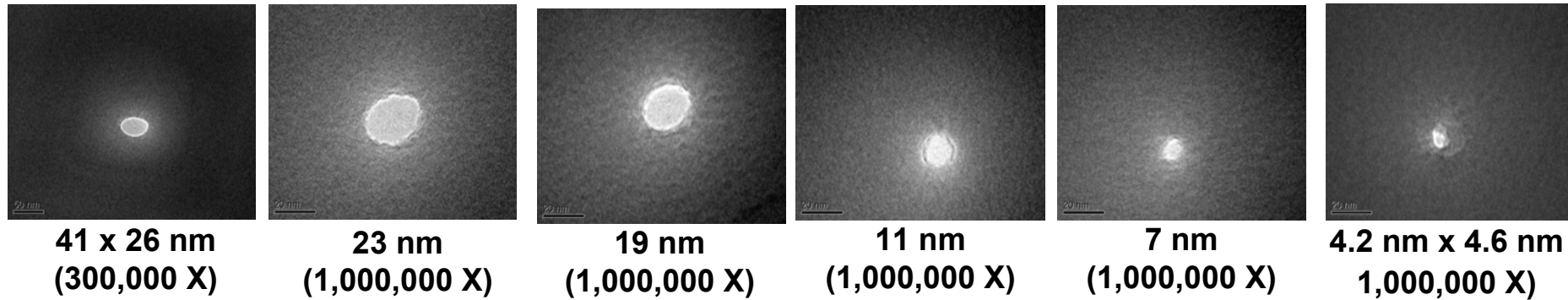


Remove buried oxide layer and regrow 100 nm thermal oxide.



Shrink the pore to 3 –5 nm by TEM

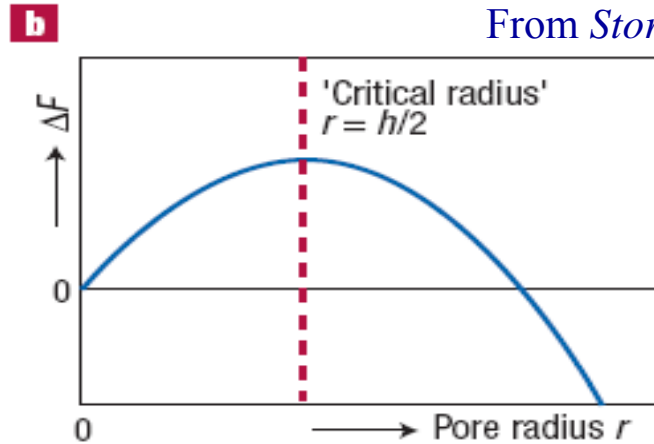
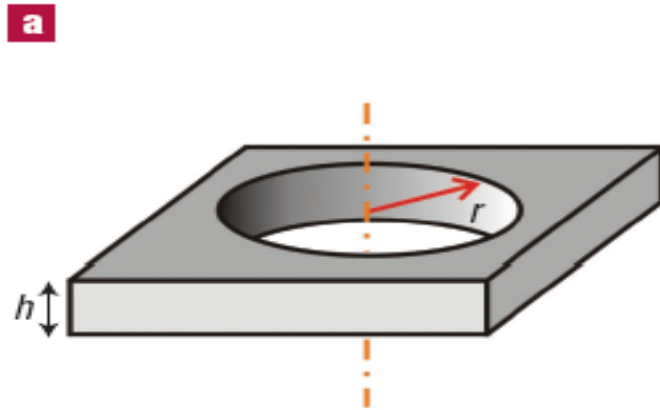
Pore shrinking and shape changing (After Thermal Oxidation, Oxide Thickness = 50 nm)



A. J. Storm, J.H. Chen, X.S. Ling, H.W. Zanderbergen and C. Dekker, "Fabrication of solid-state nanopores with single-nanometre precision", Nature Materials, 2, 537 (2003).

H. Chang, F. Kosari, G. Andreadakis, G. Vasmatzis, E. Basgall, A. H. King, and R. Bashir, "Towards Integrated Micro-Machined Silicon-Based Nanopores For Characterization Of DNA", Hilton Head MEMS conference, 2004, Hilton Head, South Carolina.

Explanation – Minimization of Surface Energy



From Storm et. al. 2003

Surface free energy:

$$\Delta F = \gamma \Delta A = 2\pi\gamma(rh - r^2)$$

where γ is the surface tension of the fluid,
 ΔA is the change in surface area.

r is the radius of the pore right after the
 final oxidation,

h is oxide thickness.

The shrinkage/expanding of pores with different radii and oxide thicknesses.

Sample name Shrinkage/Expansion (S/E)	Average radius of the pore r (nm)	Grown oxide thickness d (nm)	The ratio of r/d
103003_4 S	9	79	0.11
102503_4 S	38	100	0.38
110603_2 S	51.5	130	0.40
091603_6m E	82	90	0.91
082703_5m E	138	120	1.15
091603_7m E	110	54	2.04

H. Chang, F. Kosari, G. Andreadakis, G. Vasmatzis, E. Basgall, A. H. King, and R. Bashir, "Towards Integrated Micro-Machined Silicon-Based Nanopores For Characterization Of DNA", Hilton Head MEMS conference, 60 2004, Hilton Head, South Carolina.

Integrated Optical Detection

